

Variable Stars in the Unusual, Metal-Rich Globular Cluster NGC 6441

Barton J. Pritzl^{1,2} and Horace A. Smith

Dept. of Physics and Astronomy, Michigan State University, East Lansing, MI 48824

e-mail: pritzl@pa.msu.edu, smith@pa.msu.edu

Márcio Catelan³

University of Virginia, Department of Astronomy, P.O. Box 3818, Charlottesville, VA
22903-0818

e-mail: catelan@virginia.edu

and

Allen V. Sweigart

NASA Goddard Space Flight Center, Laboratory for Astronomy and Solar Physics,
Code 681, Greenbelt, MD 20771
e-mail: sweigart@bach.gsfc.nasa.gov

Received _____; accepted _____

Draft, 07/16/01 – v12.2

¹Visiting Astronomer, Cerro Tololo Inter-American Observatory, National Optical Astronomy Observatories, which is operated by AURA, Inc., under cooperative agreement with the National Science Foundation.

²Current address: National Optical Astronomy Observatories, P.O. Box 26732, Tucson, AZ 85726, email: pritzl@noao.edu

³Hubble Fellow.

ABSTRACT

We have undertaken a search for variable stars in the metal-rich globular cluster NGC 6441 using time-series BV photometry. The total number of variables found near NGC 6441 has been increased to ~ 104 , with 48 new variables being found in this survey. A significant number of the variables are RR Lyrae stars (~ 46), most of which are probable cluster members. As was noted by Layden et al. (1999), the periods of the fundamental mode RR Lyrae are unusually long compared to field stars of similar metallicity. The existence of these long period RRab stars is consistent with Sweigart & Catelan's (1998) prediction that the horizontal branch of NGC 6441 is unusually bright. This result implies that the metallicity-luminosity relationship for RR Lyrae stars is not universal. We discuss the difficulty in determining the Oosterhoff classification of NGC 6441 due to the unusual nature of its RR Lyrae. A number of ab-type RR Lyrae are found to be both brighter and redder than the other probable RRab found along the horizontal branch, which may be a result of blending with stars of redder color. A smaller than usual gap is found between the shortest period fundamental mode and the longest period first-overtone mode RR Lyrae. We determine the reddening of the cluster to be $E(B-V) = 0.51 \pm 0.02$ mag, with substantial differential reddening across the face of the cluster. The mean V magnitude of the RR Lyrae is found to be 17.51 ± 0.02 mag resulting in a distance of 10.4 to 11.9 kpc, for a range of assumed values of $\langle M_V \rangle$ for RR Lyrae stars. The possibility that stars in NGC 6441 may span a range in [Fe/H] is also discussed.

Subject headings: Stars: variables: RR Lyrae stars; Galaxy: globular cluster: individual (NGC 6441)

1. Introduction

Armandroff & Zinn (1988) determined the metal abundance of NGC 6441 to be $[\text{Fe}/\text{H}] = -0.53 \pm 0.11$, making it slightly more metal-rich than 47 Tucanae on their metallicity scale. One might therefore have expected that the color-magnitude diagram (CMD) of NGC 6441 would show the stubby red horizontal branch (HB) typical of metal-rich globular clusters such as 47 Tuc. The CMD of NGC 6441 does indeed show a strong, red HB component, but Rich et al. (1997), using *Hubble Space Telescope* (HST) observations, discovered that the CMD of NGC 6441 also has a pronounced blue HB component, which stretches across the location of the instability strip. Not only does the HB have a blue component, but it also slopes upward as one goes blueward in a $(V, B-V)$ CMD. NGC 6441 is not, however, unique in these characteristics: Rich et al. showed that the CMD of the relatively metal-rich globular cluster NGC 6388 has a similar HB morphology. It has long been known that the HB morphology of globular clusters does not correlate perfectly with $[\text{Fe}/\text{H}]$ and that at least one parameter besides $[\text{Fe}/\text{H}]$ is needed to account for this (Sandage & Wildey 1967; van den Bergh 1967). NGC 6441 and NGC 6388 are the only metal-rich globular clusters known to exhibit this second parameter effect.

Sweigart & Catelan (1998) constructed CMD simulations of metal-rich globular clusters to test various theoretical scenarios which might account for the unusual HB morphologies in NGC 6441 and NGC 6388. They found that the upward slope of the HBs could not be explained by differences in either cluster age, mass loss on the red giant branch (RGB), or differential reddening. Layden et al. (1999) would later, on observational grounds, also rule out the hypothesis of differential reddening. Sweigart & Catelan did arrive at three theoretical scenarios for explaining the HB morphology: (1) a high cluster helium abundance; (2) a rotation scenario in which rotation during the RGB phase increases the HB core mass; and (3) a mixing scenario, in which deep mixing on the RGB enhances the

envelope helium abundance. All three of these scenarios predict that any RR Lyrae stars (RRLs) in NGC 6388 and NGC 6441 should be anomalously bright. Although at the time little was known about RR Lyrae stars in NGC 6441, the few RR Lyrae stars known in NGC 6388 had properties which were consistent with an unusually high luminosity (ref. Fig. 3, Sweigart & Catelan 1998).

Sweigart (1999) suggested an additional scenario: Some stars might form dust grains which are then removed from the envelope by radiation pressure at the tip of the RGB, leaving behind metal-depleted gas. The overall metal abundance of the envelope might then be reduced if the metal-depleted gas can be convectively mixed throughout the envelope. One would then expect an HB star that has undergone such metal-depletion to be both bluer and brighter than would otherwise be the case. As a variation of this metal-depletion scenario, Sweigart (2001) suggested that the unusual HB morphology in NGC 6441 and NGC 6388 might also be due to an intrinsic spread in metallicity among the stars in these clusters, a possibility first noted by Piotto et al. (1997). Detailed stellar evolution calculations have shown that a metallicity spread can produce upward sloping HBs similar to those observed in these clusters (Sweigart 2001). Under this scenario NGC 6441, along with NGC 6388, would be metal-rich analogs of ω Centauri, the only Galactic globular cluster known to contain a spread in metallicity.

Layden et al. (1999) used ground-based V and I photometry of NGC 6441 to study its CMD and its variable star population. They discovered about 50 new variable stars in the vicinity of NGC 6441, including 11 RRLs which they believed to be probable members of the cluster and 9 other suspected cluster variables, 6 of which were candidate RRLs. The RRab stars which they believed to be probable members had unusually long periods. Their locations in the period-amplitude diagram (ref. Figure 9, Layden et al. 1999) were consistent with the models of Sweigart & Catelan (1998), implying that the RRLs were

indeed unusually bright. Layden et al. also found a value of 1.6 for the ratio R of HB stars to RGB stars, implying that the helium abundance of NGC 6441 is not extraordinarily high. Thus, the high helium scenario seems to be effectively ruled out.

This paper reports new B and V photometry of NGC 6441 which has led to the discovery of additional variable stars. Preliminary results from these observations have already been used to argue that the RRLs in NGC 6441 are unusually bright for the cluster metallicity (Pritzl et al. 2000). Here we present the results of the new study in detail and call attention to several unusual properties of RRLs in NGC 6441. The results for NGC 6388 will be reported in a separate paper (Pritzl et al. 2001).

2. Observations and Reductions

Time series observations of NGC 6441 were obtained at the 0.9 m telescope at Cerro Tololo Inter-American Observatory using the Tek 2K No. 3 CCD detector with a field size of 13.5 arcmin per side. Time series observations of NGC 6441 were obtained on the UT dates of 1998/May/26-29 and 1998/June/1-4. Exposures of 600 seconds were obtained in both B and V filters. The seeing ranged from 1.1 to 2.5 arcsec, with a typical seeing of 1.4 arcsec. Images were centered 4 arcmin east of the cluster center, to avoid including a bright foreground star within the field.

Twilight sky flats were taken on nights 1, 2, 4, 5, and 6. The sky flats were examined for any nightly variations and no significant variations were detected. The sky flats were then combined into one master sky flat that was used for each frame. Corrections for bias and flat fielding were done using conventional IRAF routines.

A total of 23 photometric standards from Landolt (1992) and Graham (1982) were observed on June 1, 2, and 3. They were typically observed four times during the night.

These primary standard stars spanned a color range from $B-V = 0.024$ to 2.326 mag, adequate to cover the color range of the reddened stars in NGC 6441. Primary standards were observed between airmasses 1.035 and 1.392. According to the CTIO sky condition archive (http://www.ctio.noao.edu/site/phot/sky_conditions.html), only the night of June 1 was photometric, but standards observed on the nonphotometric nights were incorporated in the reductions using the “cloudy” night reduction routines created by Peter Stetson (private communications). This allowed us to make use of a broader range of colors from the primary standards observed on the other nights to better define the color terms in the transformation equation.

Photometry of stars in the NGC 6441 field was obtained using the standalone reduction packages created by Stetson (1994): DAOPHOT II, ALLSTAR, and ALLFRAME. Point-spread functions (PSF) were calculated for each frame from a set of 80 bright, uncrowded stars, using the variable PSF option. Instrumental magnitudes v and b for the NGC 6441 stars were transformed to Johnson V and B magnitudes using Stetson’s TRIAL package. Thirty nine local standards within the NGC 6441 field were used to set the frame-by-frame zero-points for the cluster observations. Because NGC 6441 was observed to higher airmass than the Landolt (1992) and Graham (1982) standards, the local standards were also used to check the adopted values of the extinction coefficients for the night of June 1. The observations of the local standards confirmed the values of the extinction coefficients determined from the primary standards. Transformation equations derived from the standard stars had the form:

$$v = V - 0.006(B-V) + 0.159(X - 1.25) + C_V \quad (1)$$

$$b = B + 0.105(B-V) + 0.243(X - 1.25) + C_B \quad (2)$$

where X is the airmass and C_V and C_B are the zero point shifts for their respective filters. Comparing the transformed magnitudes of the standard stars with the values given by Graham and Landolt, we find rms residuals of 0.018 magnitudes in V and 0.006 magnitudes in B .

The photometry of stars in the NGC 6441 field could be compared with photometry in three earlier studies, as shown in Table 1. First, our B and V photometry was compared with the HST B , V photometry obtained by Rich et al. (1997). Unfortunately, even the outermost stars in the field of view of WFPC2 tended to be crowded on the images obtained at CTIO. The comparison with Rich et al. is therefore based upon only 13 stars for which the crowding on our images, although still significant, is small enough to allow a meaningful comparison. Our ground-based photometry is brighter in V by about 0.04 mag. No significant difference in B is evident.

A larger number of comparisons could be made with the photoelectric and photographic photometry of Hesser & Hartwick (1976). In Figure 1 we show the differences between our results and the local standards established by Hesser & Hartwick. At low $B-V$, there is some scatter, but the mean differences are small. The results are more discordant for the reddest stars. Excluding stars with $B-V > 2.0$ mag, we obtained the results listed in Table 1. Our mean V and B values are slightly brighter than those of Hesser & Hartwick by an amount smaller than or comparable to the standard error of the mean. We are not certain of the origin of the greater discrepancy for very red stars, though we note that these more discrepant stars tended to be among the fainter as well as the redder stars used in the comparison. Our inclusion of a second-order color term in our transformation equations produced no significant decrease in the discrepancy at larger $B-V$ values. It is noteworthy that Figure 1 shows no trend with $B-V$ for the bluer colors relevant to the region of the RRLs. No trend with color was seen in the comparison of our results with the HST

photometry.

Finally, we compared our V magnitudes with the V photometry of Layden et al. (1999). As indicated in Table 1, our V photometry and that of Layden et al. are surprisingly discrepant. We have no good explanation for this discrepancy. The agreement between our V photometry and that of Rich et al. (1997) and Hesser & Hartwick (1976) suggests that there is a zero-point error of approximately 0.4 mag in the Layden et al. photometry.

3. Color-Magnitude Diagram

The CMD was the critical tool for the initial discovery of the unusual nature of NGC 6441. For this reason we will now compare our new CMDs with those presented by Rich et al. (1997) and Layden et al. (1999).

Figure 2 shows four CMDs obtained from our photometry for stars lying at different distances from the center of NGC 6441. A total of 14127 stars make up the CMD in Figure 2a. Only the stars with values of $\chi < 1.5$ from Stetson's TRIAL program were included. The strong red component of the HB is evident ($V \sim 18$, $B-V \sim 1.4$) as is its blue extension. We also see many features of the field bulge population, which are particularly prominent since our images are shifted off of the cluster center to avoid a foreground star. The main sequence of the field extends up through the cluster's HB from about $B-V \sim 1.2$ to ~ 0.8 mag and from about $V \sim 20$ to ~ 15.5 mag. The field red HB clump is found at $V \sim 17$ mag and $B-V \sim 1.7$ mag. The contribution of the bulge stars to the CMD of Figure 2a can be seen in Figure 2d, where we have plotted all stars that are 6-11 arcmin eastward from the cluster center [the tidal radius of NGC 6441 extends to 8.0 arcmin (Harris 1996)].

One interesting feature on the diagrams of NGC 6441, which can also be seen in the

CMDs of Rich et al. (1997) and Layden et al. (1999), is a small clumping of stars slightly fainter and redder than the red HB of NGC 6441 ($V \sim 18.5$, $B-V \sim 1.4$). This appears to be the RGB luminosity function bump. Although this bump is difficult to discern in Figure 2, its presence in the HST CMD makes it likely to be associated with the cluster. An investigation into its properties might constrain the helium content of the cluster (Sweigart 1978; Fusi Pecci et al. 1990; Zoccali et al. 1999; Bono et al. 2001).

Figure 2b is our closest approximation to the area covered by the CMD of Rich et al. (1997), including stars within a radius extending out to approximately 1.7 arcmin from the cluster center. The morphology of the HB is clearer in this figure and Figure 2c. Not only do we see the sloped nature of the blue extension to the HB, but the slope in the red HB is also seen as was first noted by Piotto et al. (1997). The HB slopes from $V \sim 18$ mag, at $B-V \sim 1.4$ mag, to $V \sim 17.5$ mag, at $B-V \sim 0.6$ mag.

Rich et al. (1997) mentioned that there may be a hint for a bimodal distribution of the stars on the HB of NGC 6441. There appears to be a gap ranging in color from 1.0 to 0.4 mag in their Figure 1. Such a bimodality is not seen in our CMDs, although field stars and differential reddening may be filling in any gap in the HB. It is possible that this gap may be due to the RRL being plotted at their instantaneous magnitudes instead of their time averaged magnitude and color in the Rich et al. CMD. Looking at our Figure 4, it is seen that the RRL fill in the HB in that region.

4. Variable Stars

4.1. Discovery of New Variable Stars

Variable stars were identified in two ways: first, Stetson's DAOMASTER routine was used to compare the rms scatter in our photometric values to that expected from the

photometric errors returned by the ALLFRAME program. Second, we applied the variable star search algorithm presented by Stetson (1996). Results from the two approaches were very similar.

The time coverage of our observations is well suited for the discovery of short period variability, but not for the detection of long period variables. All of the probable short period variable stars identified by Layden et al. (1999) which were within our field were recovered during our variable star searches. In addition, 48 probable new variable stars were detected, along with 6 suspected variables. In crowded regions close to the cluster center, the B photometry proved superior to the V photometry for purposes of identifying variable stars, presumably because of the lesser interference from bright red giant stars. Finding information for the new variable stars is given in Table 2, where X , Y are the coordinates of the variables on the CCD [the cluster center is assumed to be at (1635,1051)] and $\Delta\alpha$, $\Delta\delta$ are the differences in right ascension and declination from the cluster center (in arcsec). Finding charts for the variables, excluding the long period variables, can be seen in Figure 3.

4.2. RR Lyrae stars

The number of probable RRL stars in the NGC 6441 field has been increased from 11 to 46. The location of these stars within the CMD is shown in Figure 4. All previously known cluster RRL have been rediscovered except for Layden et al.’s (1999) V36, a field star lying outside the field of our observations. Table 3 lists the mean properties of the individual RRL stars found in this survey, along with one δ Scuti or SX Phoenicis star. All periods were found using the phase dispersion minimization program in IRAF. The accuracy of these periods is ± 0.001 d to ± 0.002 d, depending on the scatter and completeness of the light curve. The periods determined for the known RRL are in good agreement with those

found by Layden et al. Magnitude weighted and luminosity weighted mean magnitudes were calculated using spline fits to the observations. The listed $\langle V \rangle$ values are luminosity weighted, but the colors are magnitude weighted, $(B-V)_{\text{mag}}$. Light curves and photometry for the variable stars in V and B are given in Figure 5, Table 4 and Table 5, respectively. The mean level of the NGC 6441 HB determined from the probable RRL members, excluding the brighter and redder RRab (see §4.4) and RRL with uncertain classification, is $V = 17.51 \pm 0.02$ mag.

As was noted by Layden et al. (1999), it can occasionally be difficult to distinguish RRc variables from eclipsing binary stars which have periods twice as long. This is particularly true for a cluster such as NGC 6441, in which a significant and variable reddening makes the precise location of a variable star in the CMD an uncertain guide as to the type of the variable. Although not always decisive, inspection of the Fourier decompositon parameters of the light curves can be an aid in classifying variables, and in distinguishing RRab from RRc variables.

Fourier decompositions of the light curves were done fitting to an equation of the form:

$$mag = A_0 + \sum A_j \cos(j\omega t + \phi_j). \quad (3)$$

Plotting the Fourier parameters A_{21} vs. ϕ_{21} gives a clear distinction between RRL types (e.g. Clement & Shelton 1997), where $A_{21} = A_2/A_1$ and $\phi_{21} = \phi_2 - 2\phi_1$. Figure 6 shows a A_{21} vs. ϕ_{21} plot for the probable RRL variables in the NGC 6441 field which have clean light curves. The data are listed in Table 6. The probable RRL fall into areas of the diagram where RRab and RRc stars would indeed be expected. A clear break between the RRL types can be seen at A_{21} of 0.3 as was originally shown by Simon & Teays (1982), with the RRab falling at values greater than this and the RRc below. It should be noted that V49 falls in the same region as the other RRc variables furthering the case for its

reclassification (see §4.3). We also see how the field star V54 stands apart from the cluster variables.

Using these RRL with quality light curves as a reference, we are able to analyze the other variables found in the field of NGC 6441. Table 7 lists the Fourier values for the contact binaries and the RRL with poorer light curves and uncertain membership or classification. It is clear that the contact binaries have values of $A_{21} > 1.0$. This provides a good distinction between the RRL and the contact binaries. There is still the question of how to determine if a variable is a RRc star or a contact binary star with a period twice as long. To test this we wanted to see how the Fourier parameters of a known RRc star would compare to those of known contact binaries if it was analyzed at the longer period that it would have were it a contact binary. We performed a Fourier analysis on V70, which is clearly a RRc variable and fits in well with the other RRc in the A_{21} vs. ϕ_{21} plot, at the longer period of 0.852 d. The resulting A_{21} value, 25.90, would indicate that it was a binary star. In order to test how contact binary stars compare to known RRc stars, we also analyzed two stars that are clearly contact binary stars, V86 and V88, at the shorter periods that they would have if they were RRc stars. The data is shown in Table 8. Comparing these results to the RRc in Figure 6, the A_{21} values are a little high and the ϕ_{21} values are low. Although more tests should be done to verify this, it appears that if one analyzes a star at a RRc-type period, a true RRc star will fall among the other RRc stars in the A_{21} vs. ϕ_{21} plot, while a binary star will be offset to low ϕ_{21} values and slightly higher A_{21} values. For comparison, as stated before, the Fourier values for V49 imply that it is a RRc variable rather than a contact binary. On the other hand, the values for V81 at the shorter RRc-like period imply that it may indeed be better classified as a contact binary.

The period-amplitude diagrams for this cluster in B and V are seen in Figure 7. There are a few RRab variables whose amplitudes are low for their period. Some of these are

probably attributable to noisy photometry (V46, V52, V53, and V55), while others are due to possible blending effects (see §4.4). The Blazhko effect can also reduce the amplitudes of RRab stars, but our observations do not extend over a long enough time interval to test for the presence of this effect. Another striking feature is the lack of a significant gap between the shortest period RRab and the longest period RRc (see §5.2 and §5.4).

4.3. Notes on Individual RR Lyrae

V45 - V45 appears to stand out from the other cluster variables. The shape of the light curve indicates that the variable is of ab type. Although our data have a gap in the light curve near minimum making its magnitude and color uncertain, we were able to determine a period similar to that in Layden et al. (1999), whose phase coverage is more complete. Layden et al. list the V amplitude of the star as 0.73 mag. We estimate the amplitude to be about 0.85 mag from our data. When we place this variable in the period-amplitude diagram for the cluster (Figure 7), it clearly stands apart from the variables we feel certain are cluster members. It is our belief that V45 is a field RRL that happens to fall at nearly the same distance as the cluster.

V49 - V49 was classified by Layden and collaborators as a possible detached binary with a period of 1.010 d. Our data indicate that this variable may instead be classified as an RRc-type variable with a period one third as long. At a period of 0.335 d, our data for one night (~ 8 h) nearly complete one cycle. When the Layden et al. (1999) observations are fit to a 0.335 d period, we get a light curve similar to our own, although with some scatter. V49 lies toward the outer parts of NGC 6441. The color of the star fits well with the other cluster RRc, but it is slightly brighter. As stated in §4.2, the Fourier values for this star place it among the other RRc stars. We are unable to determine what, if any, reddening effects may be responsible for the difference in brightness. Although we believe

that V49 is more likely to be an RRc than a detached binary, more photometry of this star would be useful in making a definite determination.

V52 - This variable has a period, magnitude, and color that would classify it as being an ab-type RRL. Yet, it is interesting to note that its light curve has a more sinusoidal shape. To illustrate the difference, it is useful to compare the light curve of V52 with those of V46, whose period is slightly longer, and V53, whose period is similar to V52. Both V46 and V53 exhibit a sharper rise in light to maximum, whereas V52 has a more gentle slope.

V54 - This variable is an RRab with a clean light curve. It is ~ 0.9 mag brighter than other cluster RRab variables. In addition, the location of V54 far from the cluster center indicates that it is a likely field variable. V54 may also be intrinsically fainter than the cluster RRab given its position in the period-amplitude diagram (Figure 7).

V64 - This star is blended with a close neighbor, only 1.3 arcsec away. The RR Lyrae-like periodicity shows up in the photometry of both stars, indicating that the photometry of both is probably affected by the blending. Therefore, it is likely that only one of the two stars is actually a variable. The B light curves for each star have scatter, with the amplitude of V64 being 0.95 mag and that of the neighbor being 0.60 mag. The V curves show a lot of scatter with amplitudes around 0.30 mag. The mean magnitudes for the companion star are $\langle V \rangle = 16.971$ mag and $(B-V)_{\text{mag}} = 1.378$ mag.

V67 - This variable is found only ~ 3.5 arcsec east from a much brighter star. Therefore blending was a problem for some of the nights with poorer seeing. These data points were removed from the light curve. Although its color is similar to the other RRab stars believed to be on the NGC 6441 HB, it is slightly brighter. This may be a consequence of its proximity to the bright star. It should be noted, however, that the ratio of B to V amplitude is not unusual. Its large distance away from the cluster center could indicate that V67 is a field star. Unlike V45 and V54, V67 falls along with the other probable cluster

members in the period-amplitude diagram (Figure 7).

V68 - (SV1, Layden et al.) We are still uncertain as to how to classify this variable. It appears as though the scatter in its curve comes from blending with a close companion star. Also, coma may be affecting our photometry since V68 is found near the edge of the frame. V68 is unusually bright, and if it is found to be an RRc variable, it should be considered to be a member of the field.

V69 - (SV2, Layden et al.) Even though it has an unusually long period, the light curve shape coupled with the location in the CMD indicates that V69 is a cluster RRL of c-type. (See §6.2.)

V70 - (SV4, Layden et al.) The magnitude and color of this variable, along with the shape of the light curve, indicate it is a c-type RRL.

V71 - (SV5, Layden et al.) The magnitude and color of this variable, along with the shape of the light curve, indicate it is a c-type RRL.

V73 - This variable has an uncertain classification. In the CMD, it is slightly brighter and redder than other RRc variables. The light curve shape is somewhat asymmetric, but there is also scatter to indicate that there might be some problem with blending. The distance of V73 from the cluster center is large enough to raise the possibility that it may be a field star.

V75 - This star falls among the RRc stars in the NGC 6441 CMD, but there is some scatter in its curve, especially in V , that makes its exact classification uncertain.

V76 - This is a longer period c-type RRL with a curve similar to that of V69. It appears to be fainter and redder compared to other RRc stars on the HB, which may be an effect of differential reddening.

V78 - This variable is fainter and redder as compared to the RRc stars on the HB, which may be an effect of differential reddening.

V79 - V79 is an RRc star as indicated by its B light curve. The V light curve has a lot of scatter in it, and the $B-V$ color for this variable, which is somewhat redder than the other RRc stars, is uncertain for that reason.

V80 - (SV3, Layden et al.) Our light curves for this star show that it is better classified as a binary rather than an RRc star. The location of this star in the CMD, which puts it in the vicinity of the RRab stars, also indicates that the star is not a c-type RRL.

V81 - A probable eclipsing binary star, but the phase coverage is not complete when plotting the longer period of 0.856 d making the classification uncertain.

V84 - This star appears to be of c-type. It is very blue as compared to the cluster RRc. There is a lot of scatter in the curves, especially in the V light curve. The mean $B-V$ color is probably unreliable.

V93 - The scatter found in the light curve of this variable makes it difficult to classify. It has a slightly asymmetric V light curve. The placement of V93 along with the other RRc variables along the horizontal branch suggests that it is a RRc variable.

V94 - This variable falls along the horizontal branch, although it is slightly redder than most of the RRc variables. The light curve shows an unusual shape having a longer than usual rise time. The precise classification of this variable is uncertain. We were unable to test if this star is a RRc star or a contact binary as in §4.2 due to the scatter in its light curve.

V95 - From the shape of the curve, the location in the CMD, and its period, this star is a foreground δ Scuti or SX Phoenicis star.

V96 - The somewhat asymmetric light curve and period of this variable indicate that it could be an RRab variable. It is difficult to make an exact determination of the variable type due to scatter found in the light curve and a gap present during the rise in the light curve. The location of this variable, slightly fainter and redder than other RRab variables, may be an effect of differential reddening.

V97 - The period found for this variable is similar to those found for other RRab variables of NGC 6441. The *B* data show definite variability with a period of 0.844 d, while the *V* data show large scatter. We have not given it a definitive classification since we see no clear minimum in the light curve.

V102 - The classification of this star is uncertain. Although the *B* light curve looks to be that of a c-type RRL, V102 is much brighter and redder than the other c-type RRL found in NGC 6441. The *V* light curve has more scatter in it than the *B* light curve, implying, as with the red RRab, that blending may be the cause of the difference (see §4.4). The *V* amplitude for this star, as is, would be at most ~ 0.1 mag.

SV6, SV7, & SV9 - Two of these suspected variables, SV6 and SV7, from Layden et al. (1999) did not show any variation in our data. Layden and collaborators designate these stars as possible long period variables (LPVs). Since our survey was not geared to search for LPVs, these stars may indeed be varying over a larger time scale than we were able to sample. SV9 was not in our field of view.

4.4. “Red” RR Lyrae

Layden et al. (1999) noted that V41 and V44 stood apart from the other cluster RRL in that they were both brighter and redder than the expected red boundary of the RRL instability strip. With the increased number of RRL found in this survey, we also found an

increased number of these unusual RRL. V62 and V65 are both brighter by approximately 0.61 mag and redder by approximately 0.25 mag in $B-V$ than typical NGC 6441 RRab stars.

Layden et al. (1999) suggested that these stars were variables with unresolved red stars contaminating their photometry. This seems the most likely explanation. NGC 6441 has a very high central stellar density, indicating that crowding effects are highly likely. A consequence of blending with a red star would be an unusually high ratio of the B to V amplitude. This indeed seems to be the case for V41, V44, V62, and V65. Several other possible “red” RR Lyrae stars were noted, but they all had large scatter in their V light curves. It should also be noted that the V light curves of these variables tended to exhibit a higher scatter than the B light curves. If the unusual color of these stars is to be explained by unresolved companions, it is perhaps unexpected that all four such stars are of type ab and none of type c, with the possible exception of V102. On the other hand, it would be easier to discover blended variables with larger amplitude, all else being equal, which might favor blends involving RRab stars.

We attempted to search the Rich et al. (1997) images for the “red” RRL and other RRL whose V light curves had large scatter to investigate if there were any nearby neighbors. We only found 8 variables that were within the field of the HST images. V56, V63, V64, V65, V75, V84, and V102 all had from 1 to 3 stars within a 0.5 arcsec by 0.5 arcsec area centered on each variable. V66 had a neighboring star within a radius of 1.2 arcsec. Only V97 did not appear to have a neighboring star. This indicates that Layden et al.’s (1999) assertion that these variables are having their photometry contaminated by unresolvable stars in the ground-based images may be correct.

4.5. Reddening

Sturch (1966) found that near minimum light the blanketing-corrected and reddening-corrected color were a function only of period, P , for RRab stars. The observed color during this phase could therefore be used in determining the reddening of an RRab star. Blanco (1992) modified Sturch’s procedure by incorporating the metallicity indicator ΔS . He found

$$E(B-V) = \langle B-V \rangle_{\phi(0.5-0.8)} + 0.0122 \Delta S - 0.00045 (\Delta S)^2 - 0.185 P - 0.356. \quad (4)$$

To infer ΔS for the NGC 6441 variables, we used two different methods. The calibration of Blanco (1992), which makes use of abundances from high resolution spectra of RR Lyrae stars, gives:

$$[\text{Fe}/\text{H}] = -0.02(\pm 0.34) - 0.18(\pm 0.05) \Delta S. \quad (5)$$

Suntzeff et al. (1991) based their alternative calibration upon the globular cluster metallicity scale adopted by Zinn & West (1984). They found:

$$[\text{Fe}/\text{H}] = -0.408 - 0.158 \Delta S. \quad (6)$$

Taking the value of $[\text{Fe}/\text{H}] = -0.53$ (Armandroff & Zinn 1988) and calculating the ΔS value, we find that the Suntzeff et al. (1991) calibration gives colors which are ~ 0.02 mag bluer than those given by the Blanco (1992) calibration. Reddenings derived from Clementini et al.’s (1995) recalibration of the delta-S index are within 0.01 mag of those obtained with the Blanco calibration, being slightly larger. Table 9 gives our

reddening determinations for RRab variables with good light curves using the Blanco calibration. Some variables had not yet achieved minimum light in the 0.5-0.8 phase range after maximum light. The points in this range were averaged to find $\langle B-V \rangle$ in all cases. The reddenings found in this way for the stars labeled as “bright and red” may be incorrect, since those stars may in fact be unresolved blended images, as noted above. The mean reddening value for the remaining 10 RRab stars which are believed to be probable members of NGC 6441 is $E(B-V) = 0.51 \pm 0.02$ mag. The range in reddening values is consistent with previous determinations (see Layden et al. 1999) that the NGC 6441 field is subject to significant differential reddening.

Also shown in Table 9 is a comparison to the reddening values found by Layden et al. (1999). We see that our reddening determinations are generally higher than those found by Layden et al. The mean reddening value determined from the six normal RRab stars observed by Layden et al. is $E(B-V) = 0.45 \pm 0.02$ mag. It is uncertain to what extent this difference arises from the discrepancy in the V magnitudes between our data and theirs since we have no way to compare with their I data in order to check their calibration of $E(V-I)$ to $E(B-V)$. Our mean reddening value for NGC 6441 can also be compared to the result of Hesser & Hartwick (1976), who determined $E(B-V) = 0.46 \pm 0.15$ mag, and the results of Zinn (1980) and Reed et al. (1988), who obtained $E(B-V) = 0.47$ and 0.49 mag, respectively, from their analyses of the integrated cluster light.

Adopting $A_V = 3.2$ $E(B-V) = 1.63$ and a range of +0.8 to +0.5 for M_V , we find the distance modulus for NGC 6441 in the range 15.08–15.38, given $V_{RR} = 17.51$. The distance to the cluster is estimated to be from 10.4 to 11.9 kpc. In comparison, Layden et al. (1999) estimated the distance to the cluster to be 11 to 13 kpc. Harris (1996) lists NGC 6441 as having a distance of 11.2 kpc with $E(B-V) = 0.44$.

Heitsch & Richtler (1999), in an analysis of NGC 6441, found the total reddening to

be $E(V - I) = 0.49 \pm 0.03$ with a maximum differential reddening of $\Delta[E(V - I)] = 0.20$. Layden et al. (1999) found $E(V - I) = 0.577$ based on the average RRL reddening. This difference may be again attributable to the zero point offset we found in the V data of Layden et al. (see §2). In comparing the V, I color-magnitude diagram of Layden et al. to Heitsch & Richtler, we see that the HB is offset to a brighter magnitude for Layden et al. Heitsch & Richtler found $V_{\text{HB}} = 17.51 \pm 0.07$, which is also in good agreement with our determination from the RRL. With these data they determined the distance to NGC 6441 to be 13.8 ± 1.3 kpc. The difference between our distance determination and theirs can be found in the adopted metallicity for NGC 6441 and in the reddening which in turn affects the adopted extinction.

One should note that the ab-type RRL in NGC 6441 by their very nature are different from those which Blanco used in establishing his relationship between metallicity, period, and intrinsic color. We have assumed here that his formula is applicable to the RRab stars in NGC 6441. This might not be the case. Bono et al. (1997) have argued on theoretical grounds that the red edge to the instability strip might lie at lower effective temperatures for metal-rich than for metal-poor RRLs of equal luminosity. If so, and if, as argued in this paper, the RRab stars in NGC 6441 are unusually bright for their metallicity, then Blanco's reddening calibration might not apply perfectly to the RRab stars in NGC 6441.

We would also like to point out that we have assumed that the RRL in NGC 6441 are metal-rich in our calculation of the reddening. If the RRL are metal-poor (see §5.5), the derived reddening would be even higher. If one assumes $[\text{Fe}/\text{H}] = -2.0$ for the RRL, the derived reddening increases by 0.05 mag, which would be much redder than the other derived reddenings for NGC 6441.

We note that the COBE/DIRBE dust maps of Schlegel, Finkbeiner, & Davis (1998) imply a high reddening $E(B - V) \simeq 0.66$ mag for NGC 6441. There is evidence suggesting

that the Schlegel et al. maps do overestimate the reddening for highly reddened regions (Arce & Goodman 1999; von Braun & Mateo 2001). Our reddening value for NGC 6441 clearly supports this conclusion.

4.6. Eclipsing Binaries and LPVs

We were able to find a number of eclipsing binary stars within our field of view, which are not likely to be members of NGC 6441. The binaries listed by Layden et al. (1999) were all recovered. Table 10 lists photometric data for the binary stars. Due to our sampling it was somewhat difficult to determine accurate periods for detached binaries.

Our observations were not geared toward locating LPVs, but we were able to detect some stars exhibiting luminosity changes over our 10 day run. These stars and their locations are listed in Table 2. We were able to reidentify a small number of LPVs already found by Layden et al. (1999) (V1, V2, V5, V6, V9, and V10) along with a couple of probable new LPVs (V98 and V99).

4.7. Suspected Variable Stars

Following the naming scheme by Layden et al. (1999), we list in Table 11 stars which exhibit variability, but were difficult to classify for reasons such as high scatter in the light curves or abnormally low amplitudes. SV10, SV11, and SV12 all show some structure to their light curves giving an indication they may be short period variables (see Figure 5). Yet, the scatter in the curves matched with their low amplitudes, ranging from 0.10 to 0.15 mag in *B* and *V*, make them difficult to classify. SV13 appears to vary in magnitude over a period of days yet the amplitude found is only 0.15 mag. The photometry of both SV14 and SV15 shows that the magnitudes of the stars have an amplitude of about 0.4 mag.

Again, scatter in the curves makes the classification of these stars unknown.

5. Discussion

5.1. General Properties of NGC 6441 RR Lyrae

The higher number of RRL now found in NGC 6441 gives us the opportunity to better analyze the properties of this cluster. In Table 12, we list the average properties of the RRL found in NGC 6441 and compare it to the clusters M3 and M15, typical Oosterhoff I and II clusters. As was shown in Layden et al. (1999) and Pritzl et al. (2000), the RRL in NGC 6441 have unusually long periods for a metal-rich globular cluster. Clusters as metal-rich as NGC 6441 usually have few if any RRL stars. If indeed such a cluster did have numerous RRLs, then, from what is known of metal-rich field RRLs, one would expect the mean period of its RRab stars to be even shorter than those of Oosterhoff type I globular clusters. In actuality, the long mean periods of the RRL in NGC 6441, and its high N_c/N_{RR} ratio (where N_c is the number of RRc stars and N_{RR} is the total number of RRL in the system), are closer to the values expected in a metal-poor Oosterhoff II globular cluster. The value of $\langle P_{ab} \rangle$ for the RRL is long even for Oosterhoff II systems.

In Figure 8, we plot the mean periods of the RRab stars in NGC 6441 and in Oosterhoff I and Oosterhoff II clusters as a function of their parent cluster metallicity, including NGC 6388 (Pritzl et al. 2001). As was shown in Pritzl et al. (2000), we see how the trend of decreasing period with increasing metallicity for Galactic globular clusters is broken by NGC 6441. We conclude, as did Pritzl et al. (2000), that NGC 6441 does not fall into either of the usual Oosterhoff groups in this diagram.

It has also been argued that evolutionary effects may be the cause of the Oosterhoff dichotomy. Clement & Shelton (1999), Lee & Carney (1999), and Clement & Rowe (2000)

have argued that the location of RRab stars in the period-amplitude diagram is more a function of Oosterhoff type rather than metal abundance. Indeed, the RRab stars in Figure 7 do fall along the line for RRab stars in Oosterhoff II clusters as given by Clement (2000; private communication).

We performed the compatibility condition test of Jurcsik & Kovács (1996) on the RRab stars in NGC 6441. The D_m values are listed in Table 6. We find that only 4 of 14 RRab stars have a value of D_m smaller than the cutoff of 5.0 suggested by Clement & Shelton (1997) as appropriate for identifying “normal” RRab light curves from Fourier fits of the order we used. The interpretation of this result in the case of the NGC 6441 variables is uncertain, however. Large values of D_m can be caused by light curves which do not have “normal” shapes, but can also result from the analysis of low quality light curves. In addition, the applicability of the D_m criterion to the characterization of the very long period RRab light curves found in NGC 6441 has not been established. Because of the short time span covered by our observations, it is also possible that stars showing the Blazhko effect might not be identified as such by inspection or by the D_m criterion in our dataset. Due to these uncertainties, in the following analysis we will include NGC 6441 variables which have light curves showing little scatter and having no significant gaps, rather than include only variables with values of D_m smaller than 5.0.

Clement & Rowe (2000) also used the masses and luminosities of the RRc stars to illustrate the differences between the Oosterhoff groups. Their Table 4 shows 7 globular clusters arranged in order of increasing $\log(L/L_\odot)$ for the RRc variables, where the RRc luminosities have been determined from Fourier parameter ϕ_{31} , where $\phi_{31} = \phi_3 - 3\phi_1$. Making use of their Eqs. 2-5, which derive from Simon & Clement (1993a, 1993b), and the Fourier parameters listed in Table 6, we have calculated the masses, luminosities, temperatures, and absolute magnitudes for a small number of RRc stars in NGC 6441 (see

Table 13). Following the criteria for acceptable stars in their paper we excluded all long period RRc stars (see §5.2) since these stars were shown to have abnormally low derived masses and included only the RRc stars with an error in ϕ_{31} below a certain limit. Our cutoff for the error in the ϕ_{31} measurement was 0.50, instead of 0.20 used by Clement & Rowe, to allow a larger sampling of stars. After this restriction we only kept RRc stars with light curves having low scatter and low errors for the data points. The RRc with the best light curve was V70. Leaving out V71 and V77, for which the Simon & Clement equations yield especially low masses, we find the mean values for the RRc star mass, $\log(L/L_\odot)$, T_{eff} , and M_V are $0.47 M_\odot$, 1.65, 7408 K, and 0.79. If we were to include V71 and V77, the mean values would change to $0.44 M_\odot$, 1.65, 7403 K, and 0.79, which are not significant changes. By the criterion of either mean luminosity or mean T_{eff} , the RRc stars of NGC 6441 appear to fall among the Oosterhoff I clusters in Clement & Rowe’s Table 4. This, of course, contradicts the result obtained above from the RRab period-amplitude diagram.

It should be noted that the masses calculated for *all* of the RRc stars tend to be low. The mean mass of $0.47 M_\odot$ is about $0.02 M_\odot$ smaller than the canonical helium core mass at the helium flash (cf. Table 1 in Sweigart 1987; see also Sweigart 1994 and Catelan, de Freitas Pachaco, & Horvath 1996 for extensive discussions of possible sources of uncertainty in the helium core mass at the helium flash). It is unlikely that a star with this mass would become a RRL star. Scatter in the light curves and/or a lack of highly sampled light curves may lead to uncertainties in the Fourier decomposition. The sinusoidal shape of the light curves of the RRc stars results in large uncertainties in the ϕ_{21} and ϕ_{31} estimates due to the ϕ_2 and ϕ_3 phases being determined with low precision. While this may lead to scatter in the derived RRc parameters, it cannot account for the systematically low values for the masses. One possible reason for the low mass values could be that a problem with the zero point in the Simon & Clement (1993a, 1993b) calibration for the RRc masses exists. In any case, it appears that even in this Oosterhoff classification based on derived physical parameters

for the RRc stars, NGC 6441 has difficulty being classified as either an Oosterhoff type I or Oosterhoff type II cluster. (Further points on this classification scheme are discussed in §5.4, §5.5, and §6.) Another possible explanation for the low RRc masses is that the Fourier relations derived by Simon & Clement (1993a, 1993b) may not be applicable to the RRc in NGC 6441, especially if some noncanonical effect is responsible for the blue extension of the HB.

Given the existence of long period RRc stars in NGC 6441 (§5.2), and the unusually low masses obtained for the RRc stars with periods near 0.3 days, one might wonder if some of the shorter period RRL might be second overtone pulsators. However, the light curves for these stars appear not very different from those of shorter period RRc stars in other clusters, and the location of these stars in the A_{21} versus ϕ_{21} diagram (Figure 6) is also broadly consistent with the locations of RRc stars in other clusters. It was also shown by Clement & Rowe (2000) that potential second-overtone RRL tend to have V amplitudes less than 0.3 mag. This is not the case for the RRc stars in NGC 6441.

Parameters for the RRab stars in NGC 6441 were derived using the Jurcsik-Kovács method (Jurcsik & Kovács 1996; Kovács & Jurcsik 1997). The Fourier parameters for the RRab stars with good light curves are listed in Table 6 and were corrected to work in the Jurcsik-Kovács method which is based on a sine decomposition. Equations 1, 2, 5, 11, 17, and 22 from Jurcsik (1998) were used to calculate the parameters listed in Table 14. The values of $\log(L/L_\odot)$ and $\log T_{\text{eff}}$ were increased by 0.1 and 0.016, respectively, following the prescription in Jurcsik & Kovács (1999). The mean values for the mass, $\log(L/L_\odot)$, $\log T_{\text{eff}}$, M_V , and $[\text{Fe}/\text{H}]$ are $0.54 M_\odot \pm 0.01$, 1.66 ± 0.02 , 3.82 ± 0.01 , 0.68 ± 0.03 , and -0.99 ± 0.06 , respectively. Comparing these results to the empirical data in Figure 1 of Jurcsik & Kovács (1999), we see that the mean value of $\log(L/L_\odot)$ for NGC 6441 is about 0.05 brighter than the data from Jurcsik & Kovács at the metallicity of -0.53. This agrees with our assertion

that the RRL in NGC 6441 are unusually bright for their metallicity. While the value for the mean mass of the NGC 6441 RRab stars is consistent with the cluster metallicity, the mean value for $\log T_{\text{eff}}$ is about 0.02 lower than the data given by Jurcsik & Kovács (1999). Comparing the mean value of M_V given by the RRab parameters against the value given by Eq. 5 in Kovács & Jurcsik (1996) relating M_V to [Fe/H], the absolute magnitude given by our RRab stars is about 0.25 mag brighter, where $M_V = 0.19[\text{Fe}/\text{H}] + 1.04 = 0.94$ for $[\text{Fe}/\text{H}] = -0.53$.

Possibly the most interesting result to come out of the analysis of the RRab is the low metallicity of $[\text{Fe}/\text{H}] = -0.99$. According to Eq. 4 of Jurcsik (1995), this metallicity is actually -1.3 on the Zinn & West (1984) scale. This seems unusually low when compared to the cluster metallicity derived by Armandroff & Zinn (1988) of -0.53. There is some question as to the validity of applying the Jurcsik-Kovács method to the RRab stars in NGC 6441, given their unusually longer periods. We nonetheless note that the mean metallicity we derive in this way is close to that predicted by the HB models of Sweigart (2001), which yeilded a best fitting track for a [Fe/H] of approximately -1.4, assuming an α enhancement of $[\alpha/\text{Fe}] = +0.3$. Such a low metallicity for the RRab stars would of course imply that there is a real spread in metallicity among the NGC 6441 stars (§5.5).

As pointed out by Pritzl et al. (2000), NGC 6441 contains an unusually large number of long period ($P > 0.8$ day) RRab. Considering all candidate RRab stars believed to be members of NGC 6441, we find 38% (10 out of 26) of the RRab to have periods greater than 0.8 day. Although other clusters are known to contain long period RRL such as these, most notably ω Centauri, to our knowledge no other cluster has such a large proportion of long period RRab. This large proportion of very long period RRab stars, a property NGC 6388 shares with NGC 6441 (Pritzl et al. 2000, 2001), is thus an additional way in which NGC 6441 is distinguished from typical Oosterhoff type II clusters.

5.2. RRc Variables

Kemper (1982) showed that there are few metal-rich RRc stars in the solar neighborhood. RRLs of any type are rare in the more metal-rich globular clusters. The unusual nature of NGC 6441 gives us an opportunity to investigate c-type RRL in an environment more metal rich than those in which they are usually found, either in globular clusters or in the field. Although the periods of a few of the RRc in NGC 6441 do tend to fall at longer values, we see that $\langle P_c \rangle$, as given in Table 12, is not unusually large compared to values found in Oosterhoff II globular clusters (Sandage 1982).

The light curves of the NGC 6441 RRc stars also seem to have some distinguishing features. As the period goes to longer values, the bump seen during rising brightness tends to be found at earlier phases. For most, but not all, of the shorter period RRc we find the bump occurring at a phase ~ 0.2 before maximum while for the longer period ones, such as V69 and V76, it occurs at ~ 0.3 before maximum. Recent progress in the nonlinear, convective hydrodynamic modeling of the light curves of RRc stars (Bono, Castellani, & Marconi 2000) may soon determine the physical properties responsible for such peculiarities.

Layden et al. (1999) mentioned that the light curves of NGC 6441 RRc stars exhibit longer than usual rise times. They comment that the RRc stars of NGC 6441 have a phase interval of “rising light” between minimum and maximum brightness greater than ~ 0.5 . While the longer period RRc variables do have rise intervals around 0.5, we find that on average, most were $\sim 0.42 - 0.45$. This is in the higher end of the range listed by Layden et al. for RRc variables from the *General Catalog of Variable Stars* (Kholopov et al. 1985). There seems to be a slight trend of increasing rise time with increasing period.

Layden et al. (1999) also noted that the minima for the RRc stars may be uncharacteristically sharp, pointing to SV3 (V70). We find that SV3 is better classified as an eclipsing binary star. We do not find any unusual sharpness to the minima of the RRc

variables.

The long period of V69 results in an unusually short gap between the period of the longest period RRc star and the period of the shortest period RRab star in NGC 6441. If the RRab and RRc stars had the same mass and luminosity, and were there a single transition line in effective temperature which divided RRab from RRc pulsators, then we would expect a gap of about 0.12 between the logarithms of the periods of the longest period RRc star and the shortest period RRab star (van Albada & Baker 1973). Clearly, we do not see that, indicating that one of those assumptions may be in error. Again, however, the existence of differential reddening in the field makes it difficult to interpret the CMD at the level which one would like in addressing this point.

With a better understanding as to which stars are RRc variables, we update the histogram over period for NGC 6441 RRLs in Figure 9. As noted in Pritzl et al. (2000), the distribution of RRc to RRab stars in NGC 6441 shows that this cluster is relatively rich in RRc stars which is similar to other Oosterhoff II clusters, contradicting what one would expect from its metallicity. Again, we see how NGC 6441 stands out as anomalous when compared to other Oosterhoff clusters.

5.3. Period-Amplitude Diagram

The period-amplitude diagram provides a way to look at the general trends of the RRL in a system without having to worry about reddening. In Figure 10 we revisit the diagram presented in Pritzl et al. (2000), comparing NGC 6441 to other globular clusters and to field stars of similar metallicity (M15: Silbermann & Smith 1995, Bingham et al. 1994; M68: Walker 1994; M3: Carretta et al. 1998; 47 Tuc: Carney et al. 1993). We see, compared to the metal-rich field stars, the RRL of NGC 6441 fall at unusually long periods.

They even stand out compared to the RRL in the Oosterhoff Type II globular clusters M15 and M68. As was noted by Pritzl et al., the trend of the increasing period with decreasing metallicity for a given amplitude is broken by this cluster. It is interesting to note that the single RRab star known to be a member of 47 Tuc, V9, falls among the RRL found in NGC 6441. We also note that we have assumed in this discussion that the metal-abundance of the RRL stars in NGC 6441 is the same as that found by Armandroff & Zinn (1988) for the cluster as a whole. As of yet, we have no direct measurement of metallicity for individual RRL stars (see §5.5).

The assertion that the RRab in NGC 6441 stand out when compared to M68 and M15 seems to contradict our previous finding that the RRab of NGC 6441 fall along the line for RRab in Oosterhoff II clusters as given by Clement (2000; private communication) (see §5.1). One key to the analysis done by Clement (2000), Clement & Rowe (2000), and Clement & Shelton (1999) is to determine which variables have “normal” light curves. This was determined by the Jurcsik & Kovács (1996) compatibility condition. For example, according to this requirement, Clement & Shelton showed that only V23 and V35 in M68 had “normal” light curves. These two stars do fall along the Oosterhoff II line implying that the RRab in NGC 6441 do not stand apart when considering those stars with “normal” light curves. The case of M15 is not as easily resolved. When plotting the Oosterhoff I and II lines as given by Clement against the M15 RRab data, a few RRab stars fall near each line with a majority of them lying in-between the two lines. We have applied the compatibility test on the M15 RRab variables with the best light curves. Table 15 lists the data. Fourier parameters for the Bingham et al. (1984) data were taken from Kovács, Shlosman, & Buchler (1986). We performed the Fourier analysis on the RRab variables from Silbermann & Smith (1995). While a couple of M15 RRab with “normal” light curves are found near either Oosterhoff line, there are a few that are found between the lines. We do note that the Bingham et al. data for M15 is photographic which may lead to some discrepancies in

the amplitudes. There are also some possible uncertainties in the compatibility condition (see §5.1).

The period shift of the RRab stars in NGC 6441 relative to RRab stars of equal B amplitude in the globular cluster M3 (from Sandage et al. 1981) is about 0.08 in $\log P$. If the masses of the RRab stars in M3 and NGC 6441 were the same, from Eq. 2 of van Albada & Baker (1971) this would correspond to a difference of $\Delta \log L = 0.10$ or $\Delta M_{\text{bol}} = 0.24$. This, admittedly simplified, analysis would make the RRab stars in NGC 6441 slightly more luminous than the RRab stars within the Oosterhoff II cluster M15.

For the luminosity difference estimated in this way to become zero as a consequence of a possible mass difference, the NGC 6441 RRL masses would have to be smaller by $\Delta \log M \approx 0.12$. Taking the M3 RRL masses to be $\langle M_{\text{RR}} \rangle \approx 0.64 M_{\odot}$ (as estimated from Eq. 7 of Sandage 1993, using $[\text{Fe}/\text{H}] = -1.55$ for the cluster metallicity), this would imply $\langle M_{\text{RR}} \rangle \approx 0.48 M_{\odot}$ for NGC 6441 – which is unreasonably small, being smaller than the helium core mass at the helium flash. Yet it is similar to that found by Fourier analysis (see §5.1).

On the other hand, the Sweigart & Catelan (1998) synthetic HB's assuming $Y_{\text{MS}} = 0.23$, $Z = 0.006$ for both the canonical and the helium-mixing scenarios [the latter with the Reimers (1975) mass-loss parameter $\eta = 0.6$] imply mean masses of $\langle M_{\text{RR}} \rangle \approx 0.58 M_{\odot}$ for the NGC 6441 RRab variables. For comparison a canonical synthetic HB for an M3-like HB morphology with $Y_{\text{MS}} = 0.23$ and $Z = 0.001$ was computed following the same methods as in Sweigart & Catelan and using the HB tracks from Catelan et al. (1998), giving $\langle M_{\text{RR}} \rangle \approx 0.65 M_{\odot}$. Taking this theoretical mass difference into account, one obtains a revised luminosity difference of $\Delta M_{\text{bol}} \simeq 0.14$ mag between the RRab stars in M3 and NGC 6441, with those in NGC 6441 still being the brighter.

5.4. Comparisons to Long Period RR Lyrae in ω Centauri

Overall, the RRL stars in ω Centauri are similar in period and amplitude to those which would be found within a typical Oosterhoff type II system. Butler et al. (1978), Caputo (1981), and Clement & Rowe (2000) have noted, however, that ω Centauri might contain a few RRL similar to those in an Oosterhoff type I cluster. In addition, as noted in Pritzl et al. (2000), ω Centauri contains a number of very long period RRab stars, similar in period and amplitude to the longer period RRab stars in NGC 6441.

Here we note that ω Cen also contains a number of RRc variables of unusually long period, similar to V69 and V76 in NGC 6441. Making use of the data from Petersen (1994), we plot the Fourier parameters ϕ_{21} vs. A_{21} for ω Cen (Figure 11). A noticeable trend is exhibited here. The longer period RRc variables lie as a distinct group at shorter ϕ_{21} ($\phi_{21} \approx 2$). A similar trend towards shorter ϕ_{21} is noticeable in Figure 6 for NGC 6441. In Figure 12, we plot some of the RRc stars in ω Cen in a period-amplitude diagram. The periods and amplitudes were taken from Kaluzny et al. (1997). When there was more than one entry for a single star, the values were averaged. The [Fe/H] values come from Rey et al. (2000) and the RRc classifications were taken from Butler et al. (1978). We see that although there seems to be a trend of increasing amplitude, decreasing period with increasing metallicity, there are some longer period RRc found in the more intermediate metallicity range.

An attempt was made to search through the literature for other long-period c-type RRL in other globular clusters. One clear case was found, V70 in M3, with $P = 0.49$ d and $A_V = 0.35$ mag, which was misclassified by Kaluzny et al. (1998) as an RRab variable, but correctly identified as an RRc by Carretta et al. (1998). Another possible long-period RRc star is V76 in M5 (Kaluzny et al. 2000). Its period of 0.432544 d makes it unusually long as compared to the other RRc stars in M5. The lack of such stars in other clusters once again

demonstrates the unusual nature of NGC 6441 and NGC 6388, and provides another way in which the clusters appear to be different from typical Oosterhoff type II systems.

This suggests that the RRL variables in NGC 6441 may, perhaps surprisingly, belong to a metal-poor component similar to the one to which the long-period RRc's in ω Cen belong (see Figure 12). Again, we note that there are no direct metallicity measurements for the RRL in NGC 6441, and that, in this paper, we have hitherto assumed them to have the overall cluster [Fe/H] value.

5.5. A Metallicity Spread in NGC 6441?

Piotto et al. (1997) first noted that the RGB of NGC 6441 shows an intrinsic spread in color. After rejecting the possibility that differential reddening is the cause of the elongated, sloping HB, they remarked that “at least qualitatively, a spread in metallicity might be an appealing explanation for the anomalous HB and for the spread in the RGB.” The RRc stars in the cluster do appear to give some support to their hypothesis. While detailed calculations are needed to verify this possibility (Sweigart 2001), we also note that:

- i) Given the NGC 6441 HB number counts (Zoccali 1999, private communication), the RRL and blue HB components comprise only $\sim 15\%$ of the total HB population of NGC 6441. Therefore, if these HB components are the progeny of metal-poor RGB stars in the cluster, only a similar small fraction of metal-poor RGB stars should be present in NGC 6441 (and similarly in NGC 6388). Such a metal-poor component could presumably be fairly easily “hidden” behind the differential reddening that is present in the cluster (e.g., Layden et al. 1999);
- ii) Since the number ratio of RRc to RRab stars in NGC 6441 is more typical of Oosterhoff type II than Oosterhoff type I clusters, one might think that the usual

“evolutionary mechanism” invoked to account for the c/ab number ratios (van Albada & Baker 1973) could be at play in this cluster as well, implying that the NGC 6441 RRL variables evolve from blue to red in the CMD. Redward evolution for stars crossing the instability strip is thought to be a likely characteristic of metal-poor globular clusters with primarily blue HB’s (e.g., Lee, Demarque, & Zinn 1990), which might also imply that the blue HB plus RRL component in NGC 6441 is metal-poor;

iii) Clement (2000), adopting a strict selection criterion to include only RRab variables with “regular” light curves (Jurcsik & Kovács 1996), found that the NGC 6441 RRab stars occupy a location in the Oosterhoff type II systems (see also Fig. 7). Pritzl et al. (2000), and our updated Figure 10, show the RRab stars in NGC 6441 to be at least as long in period at a given amplitude as the RRab stars in typical Oosterhoff type II systems. That might suggest that the NGC 6441 RRab stars are metal-poor, given that the most metal-rich Oosterhoff type II systems known have $[\text{Fe}/\text{H}] \simeq -1.6$ (Ortolani et al. 2000);

iv) Moehler, Sweigart, & Catelan (1999) have shown that the gravities of the blue-HB stars in NGC 6441 (and NGC 6388) are not consistent with the predictions based on the non-canonical scenarios proposed by Sweigart & Catelan (1998). On the other hand, their measured gravities are not clearly inconsistent with canonical, metal-poor models.

Hence it appears that the Piotto et al. (1997) conjecture that a spread in metallicity would be qualitatively consistent with the anomalous HB of NGC 6441 is supported by some of the currently available data for the RRL variables and blue-HB stars in the cluster. But can a spread in metallicity lead to a sloping HB as seen in the cluster as well?

Apparently, yes. If we assume, as is currently believed, that the mean slope of the $M_V(\text{HB}) - [\text{Fe}/\text{H}]$ relation is in the range $\sim 0.2 - 0.3$, and if the more metal-rich component (i.e., the bulk) of the cluster has $[\text{Fe}/\text{H}] \approx -0.5$ dex, this would imply that the more metal-poor component of the cluster would have a metallicity of the order

$[\text{Fe}/\text{H}] \approx -2.2 \rightarrow -3.0$ dex. While this may seem somewhat too low, there are several effects which may, at least in principle, contribute to the production of an HB slope and hence alleviate somewhat the constraints on the metallicity of the metal-poor component, such as: a) An increase in the slope of the $M_V(\text{HB}) - [\text{Fe}/\text{H}]$ relation for $[\text{Fe}/\text{H}] > -1$ (e.g., Castellani, Chieffi, & Pulone 1991); b) Helium mixing and/or an increase in the core mass at the helium flash for the more metal-poor components (Sweigart 1997); c) Evolution away from a blue, metal-poor zero-age HB, which might make any evolved metal-poor RRL stars brighter than the “mean” $M_V(\text{HB}) - [\text{Fe}/\text{H}]$ relation (e.g., Lee & Carney 1999); d) A “canonical slope” of the zero-age HB (Brocato et al. 1999), which, though small ($\Delta V \simeq 0.1$ mag), would contribute to producing a sloping HB; e) Differential reddening, which is clearly present in the field of the cluster (§4.5; Layden et al. 1999).

These arguments are obviously of a qualitative nature. However, Sweigart (2001) has recently carried out stellar evolution calculations to explore this metallicity-spread scenario in more detail. These evolutionary models show that a spread in metallicity can naturally lead to an upward sloping HB under the simple assumptions that all of the stars are coeval and that the mass loss efficiency, as measured by the Reimers (1975) mass loss parameter, is independent of $[\text{Fe}/\text{H}]$. Moreover the size of the predicted HB slope is close to that observed in NGC 6441.

However, among the issues that still need to be addressed, we highlight the following possible caveats:

i) Why are NGC 6441 and ω Cen able to produce long-period RRc variables, which seem to be extremely rare in single-metallicity globular clusters (see §5.4)? Can this be somehow related to the extreme deep mixing signatures which have been identified in ω Cen (Norris & Da Costa 1995a, 1995b)? Obviously, abundance measurements are badly needed for both the red giants and HB stars in NGC 6441 (and NGC 6388);

- ii) Is the HB luminosity function of NGC 6441 consistent with a sloping HB caused by a metallicity sequence, with mean metallicity decreasing with bluer colors? Since at any given metallicity globular cluster HBs show a large spread in color, a superposition of “template” HBs of globular clusters of different metallicity (e.g., 47 Tuc at the metal-rich end, NGC 362, M3, M2, M15, all the way down to NGC 5053 at the most metal-poor end) would certainly not lead to a “tight” sloping HB, but instead to a large color/luminosity scatter at any given luminosity/color;
- iii) Following the same reasoning as above, the RRL population might also be expected to have contributions from several different metallicity values. Would this be consistent with the overall brightness of the NGC 6441 RRL? How would this be reconciled with the fairly tight period-amplitude distribution of the cluster stars?
- iv) What is the connection between the bright NGC 6441 RRL stars and V9 in 47 Tuc? While a correlation between position on the HB and mixing signatures has been clearly demonstrated in the case of 47 Tuc (Briley 1997), a spread in metallicity appears rather unlikely for this cluster (Suntzeff 1993). As a matter of fact, V9 itself has been conclusively shown to be only moderately metal-deficient (Keith & Butler 1980; Smith 1984), with a metal abundance consistent with that of 47 Tuc;
- v) If the RRL in NGC 6441 are indeed very metal poor, one would expect them to be more massive than those in Oosterhoff type I clusters (e.g., Sandage 1993 and references therein). However, our derived RR_C masses (§5.1) are very low – even lower than those derived using the same method for Oosterhoff I globular clusters such as M3, M5, NGC 6171 (cf. Table 3 in Kaluzny et al. 2000, and Table 4 in Clement & Rowe 2000) and NGC 6229 (Borissova, Catelan, & Valchev 2001). Can this trend be reconciled with the “metal-poor” scenario? On the other hand, recent work by Sohn et al. (2001) has shown that the RR_C masses derived using this method appear to be very low for the $[\text{Fe}/\text{H}] \simeq -2$, Oosterhoff II

cluster M53 (NGC 5024).

6. Classification

It has been shown throughout this paper, along with the discussion in Pritzl et al. (2000), that the classification of NGC 6441 into one or the other of the usual Oosterhoff groups is difficult. The long periods of the RRab stars and the relatively large proportion of c type pulsators are more typical of Oosterhoff II than Oosterhoff I systems, though we again note that $\langle P_{ab} \rangle$ is unusually large even for Oosterhoff II. In contrast, the mean luminosity of the NGC 6441 RRc stars as found by applying the Simon & Clement (1993a, 1993b) method (see §5.1) is consistent with values found in Oosterhoff I clusters such as M3. This is in conflict with our assertion that the RRL are unusually bright (see §5.3). Figure 7 shows that the NGC 6441 RRab stars do appear to fall along the line in the period-amplitude diagram for RRab stars in Oosterhoff II clusters, as given by Clement & Shelton (1999). However, using a somewhat different sample of comparison stars, we find in Figure 10 that the NGC 6441 stars tend to have slightly longer periods at a given amplitude than the bulk of the RRab stars in the Oosterhoff II clusters M15 and M68.

The mere fact that NGC 6441 has a blue extension to its HB that extends through the instability strip makes it unusual when compared to other metal-rich globular clusters. It may be the case that RRL that form in metal-rich globular clusters exhibit different properties than metal-rich stars that form in the field. As shown in Figure 10, V9 in 47 Tuc falls in the same region of the period-amplitude diagram as the RRab in NGC 6441 and NGC 6388. Recently, a RRab star was found in the metal-rich cluster Terzan 5 (Edmonds et al. 2001). While its period (~ 0.61 d) is shorter than the average periods of the RRab in NGC 6441 and NGC 6388 and V9 in 47 Tuc, it is longer than field stars of similar metallicities. These examples (see also Layden 1995, esp. his Fig. 1) all illustrate that

these clusters may be exceptions to the Oosterhoff classification scheme and to the usual correlation of RRL properties with metallicity among field RRL.

7. Summary and Conclusions

NGC 6441 stands out as one of the more unique globular clusters of our Galaxy. NGC 6441 is confirmed to be a metal-rich globular cluster exhibiting an unusual horizontal branch morphology. A strong red component of the horizontal branch is seen, as is expected for a cluster in this metallicity range. In addition to the red clump, the cluster has a blue horizontal branch extending through the instability strip which is not found in other clusters of similar metallicities except for NGC 6388, i.e., NGC 6441 exhibits a second-parameter effect. The explanations of such an effect may be constrained by the sloped nature of the horizontal branch, getting brighter in V with decreasing $B-V$, as Sweigart & Catelan (1998) suggested. It is also possible that NGC 6441 may have a spread in its metallicity making it analogous to ω Centauri, in which case its classification as a “second-parameter cluster” may not be strictly applicable, although this remains to be established.

The number of known RR Lyrae stars in the NGC 6441 field has been increased to 46. As predicted by Sweigart & Catelan (1998), the periods of the RR Lyrae are unusually long for a cluster of its metallicity, a result confirmed and extended in the period-amplitude diagram comparing NGC 6441 to other globular clusters. A few long period RRc stars were also found to exist in the cluster, resulting in a smaller than expected gap between the longest period RRc and the shortest period RRab stars. Such long-period RRc’s are extremely rare among globular clusters, with the notable exception of ω Centauri.

NGC 6441 was found to contain a number of fundamental mode RR Lyrae that are both brighter and redder than the other probable RRab found along the horizontal branch.

This effect is likely due to blending with unresolved red companion stars. The reddening determined for NGC 6441 is $E(B - V) = 0.51 \pm 0.02$ mag with significant differential reddening across the cluster. From the RR Lyrae in the cluster, excluding the brighter and redder RRab stars, the mean V magnitude of the horizontal branch was determined to be 17.51 ± 0.02 mag leading to a range in distance of 10.4 to 11.9 kpc.

NGC 6441 was shown to stand apart from other Galactic globular clusters in that it does not fit in the Oosterhoff classification scheme. The mean periods of the RRab in the cluster are as long as or even longer than the typical, more metal-poor, Oosterhoff Type II clusters. This contradiction in the trend of increasing period with decreasing metallicity, for a given amplitude, implies that the metallicity-luminosity relationship for RR Lyrae stars is not universal – if, in fact, the RR Lyrae stars in NGC 6441 do share the cluster's relatively high overall metallicity.

This work has been supported by the National Science Foundation under grants AST 9528080 and AST 9986943. Support for M. C. was provided by NASA through Hubble Fellowship grant HF-01105.01-98A awarded by the Space Telescope Science Institute, which is operated by the Association of Universities for Research in Astronomy, Inc., for NASA under contract NAS5-26555. A. V. S. gratefully acknowledges support from NASA Astrophysics Theory Program proposal NRA-99-01-ATP-039.

B. P. would like to thank Peter Stetson for the use of his reduction programs and his assistance in getting them to run properly. Thank you to Nancy Silbermann for sharing her knowledge of the reduction programs. Thank you to Suzanne Hawley and Tim Beers for their insightful comments. Thank you to Brian Sharpee for the use of his spline programs. We would also like to thank Christine Clement for the use of her Fourier deconvolution program, and for providing analytical formulae for her Oosterhoff lines in the period-amplitude diagram. We also thank Johanna Jurcsik for her assistance in the

preliminary Fourier parameters for the NGC 6441 variables. Thank you to the anonymous referee for the insightful comments and suggestions.

REFERENCES

Arce, H. G., & Goodman, A. A. 1999, *ApJ*, 512 L135

Armandroff, T. E., & Zinn, R. 1988, *AJ*, 96, 92

Bingham, E. A., Cacciari, C., Dickens, R. J., & Fusi Pecci, F. 1984, *MNRAS*, 209, 765

Blanco, V. 1992, *AJ*, 104, 734

Bono, G., Caputo, F., Cassisi, S., Incerpi, R., & Marconi, M. 1997, *ApJ*, 483, 811

Bono, G., Cassisi, S., Zoccali, M., & Piotto, G. 2001, *ApJ*, 546, L109

Bono, G., Castellani, V., & Marconi, M. 2000, *ApJ*, 532, L129

Borissova, J., Catelan, M., & Valchev, T. 2001, *MNRAS*, 324, 77

Briley, M. M. 1997, *AJ*, 114, 1051

Brocato, E., Castellani, V., Raimondo, G., & Walker, A. R. 1999, *ApJ*, 527, 230

Butler, D., Dickens, R. J., & Epps, E. 1978, *ApJ*, 225, 148

Caputo, F. 1981, *Ap&SS*, 76, 329

Carney, B. W., Storm, J., & Williams, C. 1993, *PASP*, 105, 294

Carretta, E., Cacciari, C., Ferraro, F. R., Fusi Pecci, F., & Tessicini, G. 1998, *MNRAS*, 298, 1005

Castellani, V., Chieffi, A., & Pulone, L. 1991, *ApJS*, 76, 911

Catelan, M., Borissova, J., Sweigart, A. V., & Spassova, N. 1998, *ApJ*, 494, 265

Catelan, M., de Freitas Pacheco, J. A., & Horvath, J. E. 1996, *ApJ*, 461, 231

Clement, C. 2000, in The Impact of Large-Scale Surveys on Pulsating Star Research, ed. L. Szabados & D.W. Kurtz (San Francisco: ASP), p. 266

Clement, C., & Rowe, J. 2000, AJ, 120, 2579

Clement, C., & Shelton, I. 1997, AJ, 113, 1711

Clement, C., & Shelton, I. 1999, ApJ, 515, L85

Clementini, G., Carretta, E., Gratton, R., Merighi, R., Mould, J. R., & McCarthy, J. K. 1995, AJ, 110, 2319

Edmonds, P. D., Grindlay, J. E., Cohn, H., & Lugger, P. 2001, ApJ, 547, 829

Fusi Pecci, F., Ferraro, F. R., Crocker, D. A., Rood, R. T., & Buonanno, R. 1990, A&A, 238, 95

Graham, J. A. 1982, PASP, 94, 244

Harris, W. E. 1996, AJ, 112, 1487

Heitsch, F., & Richtler, T. 1999, A&A, 347, 455

Hesser, J. E., & Hartwick, F. D. A. 1976, ApJ, 203, 97

Jurcsik, J. 1995, AcA, 45, 653

Jurcsik, J. 1998, A&A, 333, 571

Jurcsik, J., & Kovács, G. 1996, A&A, 312, 111

Jurcsik, J., & Kovács, G. 1999, New Astronomy Reviews, 43, 463

Kaluzny, J., Hilditch, R. W., Clement, C., & Rucinski, S. M. 1998, MNRAS, 296, 347

Kaluzny, J., Kubiak, M., Szymanski, M., Udalski, A., Krzeminski, W., & Mateo, M. 1997, A&AS, 125, 343

Kaluzny, J., Olech, A., Thompson, I., Pych, W., Krzeminski, W., & Schwarzenberg-Cerny, A. 2000, A&AS, 143, 215

Keith, D. W., & Butler, D. 1980, AJ, 85, 36

Kemper, E. 1982, AJ, 87, 1395

Kholopov, P. N. 1985, General Catalogue of Variable Stars (4th ed.; Moscow: Nauka)

Kovàcs, G., & Jurcsik, J. 1996, ApJ, 466, L17

Kovács, G., & Jurcsik, J. 1997, A&A, 322, 218

Kovács, G., Shlosman, I., & Buchler, J. R. 1986, ApJ, 307, 593

Landolt, A. U. 1992, AJ, 104, 340

Layden, A. C. 1995, AJ, 110, 2312

Layden, A. C., Ritter, L. A., Welch, D. L., & Webb, T. M. A. 1999, AJ, 117, 1313

Lee, J.-W., & Carney, B. W. 1999, AJ, 118, 1373

Lee, Y.-W., & Demarque, P., & Zinn, R. 1990, ApJ, 350, 155

Moehler, S., Sweigart, A. V., & Catelan, M. 1999, A&A, 351, 519

Norris, J. E., & Da Costa, G. S. 1995a, ApJ, 441, L81

Norris, J. E., & Da Costa, G. S. 1995b, ApJ, 447, 680

Ortolani, S., Momany, Y., Barbuy, B., Bica, E., & Catelan, M. 2000, A&A, 362, 953

Petersen, J. O. 1994, *A&AS*, 105, 145

Piotto, G., et al. 1997, in *Advances in Stellar Evolution*, ed. R. T. Rood & A. Renzini (Cambridge: Cambridge University Press), p. 84

Pritzl, B., Smith, H. A., Catelan, M., & Sweigart, A. V. 2000, *ApJ*, 530, L41

Pritzl, B., Smith, H. A., Catelan, M., & Sweigart, A. V. 2001, in preparation

Reed, B. C., Hesser, J. E., Shawl, S. J. 1988, *PASP*, 100, 545

Reimers, D. 1975, in *Mem. Soc. R. Sci. Liège* 6 Sér., 8, 369

Rey, S.-C., Lee, Y.-W., Joo, J.-M., Walker, A., & Baird, S. 2000, *AJ*, 119, 1824

Rich, R. M., et al. 1997, *ApJ*, 484, L25

Sandage, A. 1982, *ApJ*, 252, 553

Sandage, A. 1993, *AJ*, 106, 703

Sandage, A., & Wildey, R. 1967, *ApJ*, 150, 469

Sandage, A., Katem, B., & Sandage, M. 1981, *ApJS*, 46, 41

Schlegel, D. J., Finkbeiner, D. P., & Davis, M. 1998, *ApJ*, 500, 525

Silbermann, N. A., & Smith, H. A., 1995, *AJ*, 110, 704

Simon, N. R., & Clement, C. 1993a, *ApJ*, 410, 526

Simon, N. R., & Clement, C. 1993b, in *IAU Colloq. 139, New Perspectives on Stellar Pulsation and Pulsating Variable Stars*, ed. J. M. Nemec & J. M. Matthews (Cambridge: Cambridge University Press), p. 315

Simon, N. R., & Teays, T. J. 1982, *ApJ*, 261, 586

Smith, H. A. 1984, *ApJ*, 281, 148

Sohn, S., Rey, S.-C., Lee, Y.-W., & Charboyer, B. 2001, in preparation

Stetson, P. B. 1994, *PASP*, 106, 250

Stetson, P. B. 1996, *PASP*, 108, 851

Sturch, C. 1966, *ApJ*, 143, 774

Suntzeff, N. 1993, in *ASP Conf. Ser. Vol. 48, The Globular Cluster–Galaxy Connection*, ed. G. H. Smith & J. P. Brodie (San Francisco: ASP), p. 167

Suntzeff, N. B., Kinman, T. D., & Kraft, R. P. 1991, *ApJ*, 367, 528

Sweigart, A. V. 1978, in *The HR Diagram*, ed. A. G. Davis Philip & D. S. Hayes (Dordrecht: Reidel), p. 333

Sweigart, A. V. 1987, *ApJS*, 65, 95

Sweigart, A. V. 1994, *ApJ*, 426, 612

Sweigart, A. V. 1997, *ApJ*, 474, L23

Sweigart, A. V. 1999, in *Spectrophotometric Dating of Stars and Galaxies*, *ASP Conf. Ser. Vol. 192*, ed. I. Hubeny, S. Heap, & R. Cornett (San Francisco: ASP), p. 239

Sweigart, A. V. 2001, in *Highlights of Astronomy*, Vol. 12, in press (astro-ph/0103133)

Sweigart, A. V., & Catelan, M. 1998, *ApJ*, 501, L63

van Albada, T. S., & Baker, N. 1973, *ApJ*, 185, 477

van den Bergh, S. 1967, *PASP*, 79, 460

von Braun, K., & Mateo, M. 2001, *AJ*, 121, 1522

Walker, A. R. 1994, AJ, 108, 555

Zinn, R. 1980, ApJS, 42, 19

Zinn, R., & West, M. J. 1984, ApJS, 55, 45

Zoccali, M., Cassisi, S., Piotto, G., Bono, G., & Salaris, M. 1999, ApJ, 518, L49

Fig. 1.— Comparison to the Hesser & Hartwick (1976) data. The differences in magnitude are magnitudes in the present study minus the photographic magnitudes in Hesser & Hartwick (1976).

Fig. 2.— Color-magnitude diagrams for the stars located in the complete field of view (a), out to a radius of 1.7 arcmin (b) and 2.7 arcmin (c) from the cluster center, and 6-11 arcmin east of the cluster center (d).

Fig. 3.— Finding charts for the variable stars. North is down and east is left.

Fig. 4.— Color-magnitude diagram for the fundamental mode RR Lyrae (filled circles), first overtone RR Lyrae (filled squares), and suspected RR Lyrae (filled triangles) in the field of NGC 6441. The field RR Lyrae, V45 and V54 in Table 3, are represented by five-pointed stars.

Fig. 5.— Light curves of variable stars.

Fig. 6.— Fourier parameter plot using A_{21} vs. ϕ_{21} to show the distinction between RR Lyrae types. The filled circle represents the field star V54.

Fig. 7.— Period-amplitude diagram for NGC 6441 in V and B showing fundamental mode RR Lyrae (filled squares) and first overtone RR Lyrae (open squares). Fundamental mode RR Lyrae which may be blended with companions are denoted by filled circles. The field star, V54, is represented by a five-point star. An asterisk denotes the probable field RR Lyrae, V45. The line represents the Oosterhoff Type II lines as given by Clement (2000; private communication).

Fig. 8.— Mean period vs. [Fe/H] diagram showing the offset of NGC 6441 (square) from the Oosterhoff I (crosses) and Oosterhoff II (asterisks) globular clusters. Also plotted is the metal-rich globular cluster NGC 6388 (circle) using data from Pritzl et al. (2001). Data for

the Oosterhoff type I and II clusters are taken from Sandage (1993).

Fig. 9.— Period distribution histogram for the RR Lyraes in NGC 6441. The dark area is occupied by c-type RR Lyrae variables. The light area is occupied by ab-type RR Lyrae variables. Only RR Lyrae with certain classification are included.

Fig. 10.— Period-amplitude diagram for the ab-type RR Lyrae variables of NGC 6441 (filled circles) as compared to field RR Lyrae of $[\text{Fe}/\text{H}] \geq -0.8$ (asterisks), V9 in 47 Tuc (open star), M3 (open boxes), M15 (filled stars), and M68 (triangles). The smaller filled circles denote variables that are believed to be blended with companions. The open circles represent the RRab stars in NGC 6388 from Pritzl et al. (2001). The boxed area, taken from Figure 9 of Layden et al. (1999), denotes the region as predicted by Sweigart & Catelan (1998) where the RR Lyrae should be located according to a helium-mixing scenario.

Fig. 11.— Fourier parameter plot using A_{21} vs. ϕ_{21} to show the distinction between RR Lyrae types in ω Centauri.

Fig. 12.— Period-amplitude diagram for the c-type RR Lyrae in ω Centauri.

Table 1. Mean Differences in Photometry

Reference	ΔV	ΔB
HST	0.036 ± 0.023	0.003 ± 0.033
Hesser & Hartwick (photoelectric)	-0.02 ± 0.04	0.02 ± 0.04
Hesser & Hartwick (photographic)	0.00 ± 0.04	0.03 ± 0.04
Layden et al.	-0.385 ± 0.011	...

Note. — difference = reference magnitude - magnitude in present study

Table 2. Locations of Variable Stars

ID	X	Y	$\Delta\alpha$	$\Delta\delta$
V1	1514.0	1161.2	49.2	-44.3
V2	1543.2	988.5	37.5	24.2
V5	1136.0	473.8	200.1	228.5
V6	1559.6	928.4	31.0	48.1
V9	1695.5	1170.2	-23.2	-47.8
V10	1441.5	1197.1	78.1	-58.5
V37	1553.3	756.7	33.5	116.2
V38	1622.1	658.2	6.0	155.3
V39	1343.3	895.1	117.3	61.3
V40	1710.2	1189.6	-29.1	-55.5
V41	1546.0	1180.0	36.4	-51.7
V42	1637.2	817.6	0.0	92.0
V43	1523.0	911.8	45.6	54.7
V44	1598.6	1187.9	15.4	-54.8
V45	1798.8	1390.0	-64.4	-135.1
V46	1996.8	1252.3	-143.5	-80.4
V47	1452.7	1809.9	73.6	-301.7
V48	784.7	1212.0	340.3	-64.4
V49	994.8	813.5	256.4	93.7
V50	1458.4	1457.3	71.4	-161.8
V51	1273.2	611.8	145.3	173.7
V52	1723.7	833.7	-34.4	85.6
V53	1655.6	856.5	-7.3	76.6
V54	278.2	924.9	542.5	49.5
V55	1654.9	958.7	-7.0	36.0

Table 2—Continued

ID	X	Y	$\Delta\alpha$	$\Delta\delta$
V56	1694.4	988.7	-22.8	24.1
V57	1714.8	1028.7	-30.9	8.3
V58	1586.2	1055.8	20.3	-2.4
V59	1757.3	1119.4	-47.9	-27.6
V60	1626.7	1166.9	4.2	-46.5
V61	1585.4	1193.7	20.7	-57.1
V62	1630.6	1203.5	2.6	-61.0
V63	1688.0	1007.4	-20.2	16.7
V64	1736.5	1057.6	-39.6	-3.1
V65	1633.2	963.3	1.6	34.2
V66	1684.5	906.7	-18.8	56.7
V67	710.3	1157.3	370.0	-42.7
V68	1981.4	1553.1	-137.3	-199.8
V69	1162.0	1102.9	189.7	-21.1
V70	1889.2	1181.9	-100.5	-52.5
V71	1538.4	846.8	39.4	80.4
V72	1586.1	518.2	20.4	210.9
V73	283.7	635.7	540.3	164.2
V74	1469.8	1027.1	66.8	8.9
V75	1652.0	1139.2	-5.8	-35.5
V76	1349.6	1149.9	114.8	-39.8
V77	1130.4	1261.8	202.3	-84.2
V78	1205.4	1629.1	172.4	-229.9
V79	1607.6	1139.4	11.8	-35.6
V80	1203.9	1288.8	172.9	-94.9

Table 2—Continued

ID	X	Y	$\Delta\alpha$	$\Delta\delta$
V81	1509.9	382.2	50.8	264.9
V82	1801.4	619.8	-65.4	170.5
V83	866.4	743.7	307.7	121.4
V84	1753.9	1006.6	-46.5	17.0
V85	1840.5	1214.2	-81.1	-65.3
V86	1880.5	1348.5	-97.1	-118.6
V87	285.5	1438.1	539.6	-154.1
V88	592.0	1683.6	417.2	-251.6
V89	1553.9	413.2	33.2	252.5
V90	483.5	943.2	460.5	42.2
V91	1625.0	1756.8	4.9	-280.6
V92	1091.9	942.3	217.7	42.5
V93	1836.7	1002.1	-79.5	18.8
V94	1672.9	958.8	-14.2	36.0
V95	1770.4	1222.9	-53.1	-68.7
V96	1978.3	1387.7	-136.1	-134.1
V97	1823.0	1099.0	-74.1	-19.6
V98	1346.7	557.4	116.0	195.3
V99	185.7	1175.1	579.4	-49.7
V100	1323.9	371.2	125.1	269.2
V101	1006.1	126.4	251.9	366.4
V102	1736.2	1215.1	-39.4	-65.6
V103	849.1	757.1	314.6	116.1
V104	1928.0	1901.9	-116.0	-338.2

Table 3. Mean Properties of RR Lyrae

ID	Period	$\langle V \rangle$	$(B-V)_{\text{mag}}$	A_V	A_B	Comments
V37	0.614	17.546	0.839	1.17	1.55	ab
V38	0.735	17.462	0.857	0.77	1.07	ab
V39	0.833	17.673	0.970	0.70	0.95	ab
V40	0.648	17.512	0.772	1.08	1.45	ab
V41	0.749	16.726	1.197	0.41	0.75	ab
V42	0.813	17.475	0.900	0.58	0.80	ab
V43	0.773	17.529	0.960	0.60	0.80	ab
V44	0.609	16.673	1.167	0.60	1.05	ab
V45	0.503	17.375	0.814	0.87	1.07	ab, Field
V46	0.900	17.453	0.915	0.40	0.54	ab
V49	0.335	16.814	0.721	c?
V51	0.713	17.711	0.939	1.00	1.35	ab, SV8
V52	0.858	17.461	0.943	0.23	0.33	ab
V53	0.853	17.442	0.900	0.36	0.50	ab
V54	0.620	16.535	0.929	0.51	0.67	ab, Field
V55	0.698	17.523	0.701	0.97	1.25	ab
V56	0.905	16.497	1.114	...	0.64	ab
V57	0.696	17.313	0.889	0.95	1.25	ab
V58	0.685	16.868	0.840	...	0.70	ab
V59	0.703	17.508	0.787	0.92	1.22	ab

Table 3—Continued

ID	Period	$\langle V \rangle$	$(B-V)_{\text{mag}}$	A_V	A_B	Comments
V60	0.857	16.823	1.114	...	0.29	ab
V61	0.750	17.623	0.926	0.77	1.06	ab
V62	0.680	16.887	1.118	0.51	1.02	ab
V63	0.700	17.064	0.755	...	0.78	ab
V64	0.718	16.986	1.321	...	0.95	ab
V65	0.757	16.911	1.090	0.40	0.61	ab
V66	0.860	17.057	1.238	...	0.44	ab
V67	0.654	16.899	0.902	0.87	1.05	ab, Field?
V68	0.324	16.129	0.586	...	0.49	c?, SV1
V69	0.561	17.453	0.816	0.40	0.56	c, SV2
V70	0.317	17.513	0.586	0.50	0.70	c, SV4
V71	0.362	17.471	0.726	0.48	0.65	c, SV5
V72	0.312	17.348	0.642	0.48	0.65	c
V73	0.320	16.968	0.865	0.38	0.52	c?, Field?
V74	0.317	17.578	0.705	0.50	0.65	c
V75	0.405	17.349	0.684	...	0.46	c?
V76	0.473	17.912	0.890	0.39	0.41	c
V77	0.376	17.494	0.679	0.47	0.65	c
V78	0.351	17.843	0.758	0.51	0.68	c
V79	0.417	17.228	0.890	...	0.68	c

Table 3—Continued

ID	Period	$\langle V \rangle$	$(B-V)_{\text{mag}}$	A_V	A_B	Comments
V81	0.428	17.878	0.912	0.37	0.38	Binary?
V84	0.316	17.377	0.162	...	0.38	c?
V93	0.339	17.332	0.737	0.54	...	c?
V94	0.386	17.368	0.801	0.36	0.54	c?
V95	0.090	17.611	0.652	0.55	0.67	δ Scuti or SX Phe
V96	0.856	17.664	0.947	ab?
V97	0.844	17.446	0.951	ab?
V102	0.308	15.834	1.429	...	0.32	c?

Table 4. Photometry of the Variable Stars (V)

HJD-2450000	V37		V38	
	<i>V</i>	σ_V	<i>V</i>	σ_V
966.180	17.800	0.023	17.740	0.021
959.158	17.136	0.018	17.267	0.017
959.227	17.401	0.020	17.378	0.018
960.162	17.958	0.027	17.627	0.021
961.327	17.874	0.022	17.198	0.017
961.358	17.936	0.024	17.261	0.018
962.079	18.047	0.024	17.201	0.022
962.125	17.460	0.021	17.292	0.018
962.164	16.913	0.022	17.351	0.017
962.247	17.223	0.027	17.466	0.021
962.285	17.357	0.021	17.538	0.017
962.318	17.458	0.022	17.558	0.019
962.355	17.547	0.021	17.590	0.020
965.085	17.996	0.021	17.337	0.019
965.122	18.070	0.022	17.399	0.020
965.168	17.889	0.021	17.457	0.019
965.206	17.191	0.018	17.527	0.017
965.238	16.922	0.018	17.558	0.018
965.272	17.053	0.018	17.593	0.019
965.303	17.189	0.020	17.608	0.018
965.339	17.315	0.020	17.648	0.020
966.071	17.589	0.023	17.639	0.019
966.103	17.649	0.020	17.675	0.018

Table 4—Continued

HJD-2450000	V37		V38	
	<i>V</i>	σ_V	<i>V</i>	σ_V
966.109	17.660	0.019	17.696	0.017
966.142	17.734	0.020	17.733	0.018
966.211	17.859	0.022	17.809	0.021
966.257	17.878	0.025	17.844	0.021
966.291	17.955	0.027	17.721	0.022
966.319	18.002	0.025	17.420	0.021
966.350	18.032	0.023	17.296	0.021
967.073	16.912	0.018	17.382	0.020
967.104	17.024	0.018	17.139	0.021
967.138	17.154	0.021	17.058	0.020
967.178	17.318	0.018	17.124	0.017
967.251	17.515	0.019	17.260	0.018
967.285	17.588	0.022	17.326	0.019
967.318	17.622	0.021	17.370	0.018
967.352	17.681	0.021	17.425	0.020
968.063	17.861	0.027	17.416	0.020
968.097	17.879	0.020	17.446	0.018
968.140	17.966	0.021	17.511	0.019
968.170	18.011	0.024	17.547	0.019
968.220	18.009	0.021	17.592	0.021
968.264	17.377	0.018	17.630	0.020
968.298	16.886	0.018	17.688	0.018

Note. — The complete version of this table is in

Table 5. Photometry of the Variable Stars (B)

HJD-2450000	V37		V38	
	<i>B</i>	σ_B	<i>B</i>	σ_B
966.188	18.801	0.017	18.720	0.019
959.146	17.702	0.010	17.977	0.015
960.147	18.887	0.072	18.583	0.039
961.318	18.801	0.018	17.891	0.009
961.350	18.874	0.027	17.954	0.018
962.086	19.003	0.034	17.986	0.025
962.133
962.172	17.490	0.011	18.192	0.014
962.239	17.854	0.019	18.345	0.018
962.276	18.072	0.019	18.420	0.018
962.310	18.241	0.017	18.458	0.016
962.346	18.380	0.018	18.522	0.019
965.093	18.986	0.031	18.170	0.015
965.129	19.018	0.020	18.238	0.019
965.161	18.913	0.015	18.313	0.013
965.199	18.110	0.010	18.392	0.008
965.231	17.489	0.010	18.468	0.014
965.264	17.613	0.013	18.530	0.016
965.296	17.802	0.017	18.518	0.014
965.328	18.019	0.017	18.567	0.013
966.079	18.501	0.025	18.584	0.021
966.119	18.568	0.021	18.640	0.018
966.149	18.642	0.015	18.693	0.014

Table 5—Continued

HJD-2450000	V37		V38	
	<i>B</i>	σ_B	<i>B</i>	σ_B
966.218	18.819	0.012	18.798	0.015
966.250	18.803	0.018	18.792	0.018
966.281	18.909	0.027	18.705	0.020
966.312	18.960	0.024	18.367	0.020
966.343	19.028	0.024	18.139	0.018
967.065	17.496	0.021	18.195	0.027
967.097	17.594	0.017	17.914	0.023
967.130	17.769	0.016	17.724	0.018
967.170	18.010	0.014	17.788	0.014
967.203	18.188	0.017	17.914	0.011
967.258	18.356	0.014	18.046	0.013
967.292	18.443	0.017	18.148	0.013
967.325	18.518	0.017	18.209	0.013
967.360	18.598	0.013	18.302	0.019
968.071	18.783	0.042	18.263	0.027
968.105	18.853	0.038	18.316	0.017
968.147	18.986	0.047	18.391	0.022
968.178	19.068	0.039	18.471	0.027
968.212	18.990	0.026	18.541	0.023
968.256	18.278	0.015	18.554	0.017
968.290	17.501	0.011	18.618	0.019

Note. — The complete version of this table is in the electronic edition of the Journal. The printed

Table 6. Fourier Coefficients For RR Lyrae

ID	A_1	A_{21}	A_{31}	A_{41}	ϕ_{21}	ϕ_{31}	ϕ_{41}	D_m
V37	0.397	0.525	0.320	0.187	4.330	2.362 ± 0.047	0.634	1.52
V38	0.293	0.472	0.237	0.114	4.418	2.708 ± 0.073	0.960	5.79
V39	0.282	0.424	0.154	0.071	4.604	2.952 ± 0.117	1.486	9.21
V40	0.390	0.515	0.348	0.152	4.335	2.452 ± 0.046	0.655	6.56
V42	0.239	0.414	0.118	0.053	4.658	2.903 ± 0.101	1.341	6.45
V43	0.237	0.421	0.188	0.059	4.377	2.843 ± 0.088	1.070	8.30
V49	0.180	0.074	0.037	0.027	5.071	3.402 ± 0.236	2.483	...
V51	0.360	0.509	0.291	0.147	4.391	2.842 ± 0.062	0.913	8.15
V55	0.368	0.475	0.239	0.101	4.527	2.808 ± 0.129	0.857	8.33
V57	0.326	0.529	0.330	0.156	4.370	2.623 ± 0.083	0.695	2.72
V59	0.331	0.432	0.273	0.144	4.454	2.762 ± 0.160	0.849	8.20
V61	0.285	0.460	0.200	0.095	4.473	2.811 ± 0.093	1.359	7.24
V62	0.168	0.600	0.337	0.150	4.193	2.344 ± 0.119	0.562	4.29
V65	0.124	0.550	0.267	0.083	4.269	2.353 ± 0.135	0.041	8.04
V67	0.316	0.405	0.282	0.176	4.112	2.105 ± 0.279	0.186	4.06
V69	0.178	0.175	0.157	0.052	3.037	0.353 ± 0.115	5.028	...
V70	0.264	0.096	0.052	0.041	4.185	3.561 ± 0.488	3.525	...
V71	0.226	0.015	0.072	0.045	4.094	5.443 ± 0.235	4.050	...
V72	0.244	0.105	0.036	0.024	4.097	4.055 ± 0.464	1.889	...
V73	0.203	0.108	0.091	0.036	5.102	4.054 ± 0.202	3.155	...
V74	0.242	0.088	0.070	0.038	3.845	4.478 ± 0.271	3.258	...
V76	0.247	0.235	0.316	0.206	0.464	0.053 ± 0.059	0.017	...
V77	0.233	0.112	0.052	0.035	3.526	5.579 ± 0.325	4.260	...
V78	0.260	0.083	0.034	0.049	4.023	4.959 ± 0.458	3.201	...
V79	0.211	0.158	0.197	0.123	4.181	5.063 ± 0.450	0.161	...

Table 6—Continued

ID	A_1	A_{21}	A_{31}	A_{41}	ϕ_{21}	ϕ_{31}	ϕ_{41}	D_m
V93	0.223	0.157	0.051	0.048	3.822	2.349 ± 0.578	4.923	...
V94	0.183	0.051	0.060	0.055	0.051	5.245 ± 0.671	5.203	...

Table 7. Fourier Coefficients For Binary Stars and Other RR Lyrae

ID	A_1	A_{21}	A_{31}	A_{41}	ϕ_{21}	ϕ_{31}	ϕ_{41}
V41	0.153	0.519	0.198	0.201	4.114	2.358 ± 0.126	0.464
V44	0.187	0.611	0.359	0.196	4.289	2.002 ± 0.112	0.470
V45	5.726	0.816	0.605	0.414	6.202	6.200 ± 0.003	6.166
V46	0.162	0.315	0.100	0.026	4.520	2.506 ± 0.385	1.019
V47	0.197	1.132	0.792	0.753	6.093	6.033 ± 0.139	5.894
V48	0.020	6.562	0.387	1.034	5.914	5.557 ± 0.309	5.645
V50	0.007	32.80	1.772	10.01	5.301	2.999 ± 3.482	4.283
V52	0.090	0.615	0.328	0.259	5.236	6.084 ± 0.116	0.818
V53	0.185	0.273	0.141	0.120	5.560	0.204 ± 0.141	0.530
V54	0.225	0.328	0.135	0.039	4.078	1.992 ± 0.059	6.113
V56	0.126	0.223	0.303	0.237	3.141	4.116 ± 0.418	6.055
V58	0.254	0.476	0.107	0.015	3.849	2.229 ± 0.993	2.525
V60	0.128	0.127	0.300	0.232	6.038	1.554 ± 0.170	1.681
V63	0.174	0.516	0.343	0.055	4.867	3.170 ± 0.357	0.222
V64	0.114	0.557	0.213	0.139	4.279	2.290 ± 0.171	0.508
V66	0.085	0.917	0.422	0.387	5.084	5.525 ± 0.273	0.205
V68	0.231	0.127	0.142	0.046	4.009	4.451 ± 0.448	4.510
V75	0.155	0.125	0.029	0.056	3.423	5.688 ± 1.859	1.072
V80	0.010	17.32	1.704	2.400	5.549	4.895 ± 0.599	4.644
V81	0.155	0.278	0.087	0.048	0.054	0.018 ± 0.277	2.684
V82	0.032	2.850	0.361	0.327	0.064	0.270 ± 0.337	0.002
V83	0.021	5.221	0.580	0.657	0.115	0.438 ± 0.455	0.205
V84	0.204	0.072	0.063	0.028	4.127	5.175 ± 0.862	5.770
V85	0.028	5.349	0.414	0.659	0.537	0.982 ± 0.605	0.943
V86	0.039	5.102	0.335	1.368	5.637	4.642 ± 0.738	5.070

Table 7—Continued

ID	A_1	A_{21}	A_{31}	A_{41}	ϕ_{21}	ϕ_{31}	ϕ_{41}
V87	0.031	3.102	0.141	0.343	2.420	3.393 ± 0.539	5.017
V88	0.006	33.81	1.239	6.771	0.143	0.698 ± 2.327	0.335
V89	0.030	4.511	0.173	0.691	5.505	5.406 ± 0.911	5.484
V90	0.014	9.963	1.222	1.090	0.781	0.796 ± 1.017	1.007
V91	0.021	13.64	1.588	2.989	0.840	0.938 ± 2.154	1.625
V92	0.037	3.780	0.337	0.903	5.807	0.469 ± 0.673	5.349
V95	0.209	0.283	0.075	0.078	3.951	5.885 ± 0.594	4.782
V96	0.063	1.018	1.092	0.685	4.981	3.030 ± 0.442	0.751
V97	0.126	1.054	1.056	0.884	3.960	1.276 ± 0.160	4.783
V100	0.285	0.953	0.429	0.510	5.837	5.673 ± 0.220	6.148
V102	0.042	0.287	0.056	0.144	4.737	5.587 ± 1.310	2.277
V103	0.037	2.534	0.152	0.315	5.705	5.472 ± 0.825	4.870
V104	0.045	6.661	0.117	3.180	2.064	0.224 ± 5.332	4.437

Table 8. Fourier Coefficients For Alternate Periods

ID	Period	A_{21}	ϕ_{21}
V86	0.162	0.231	0.171
V88	0.226	0.225	0.053
V49	0.335	0.074	5.071
V81	0.428	0.228	0.054

Table 9. Reddening Determinations

$E(B-V)$			
ID	Pritzl et al.	Layden et al.	Comments
V37	0.528	0.410	
V38	0.499	0.412	
V39	0.570	0.548	
V40	0.440	0.468	
V41	0.822	0.683	Bright & Red
V42	0.484	0.444	
V43	0.504	0.413	
V44	0.847	0.676	Bright & Red
V51	0.600	...	
V54	0.541	...	Field
V57	0.561	...	
V59	0.427	...	
V61	0.535	...	
V62	0.822	...	Bright & Red

Table 10. Mean Properties of Binary Stars

ID	Period	$\langle V \rangle$	$(B-V)_{\text{mag}}$	A_V	A_B	Comments
V47	0.703	16.489	0.972	1.20	1.10	Detached
V48	0.668	15.501	0.864	0.31	0.32	Contact
V50	0.433	18.183	1.138	0.52	0.60	Contact
V80	0.900	17.409	0.966	0.38	0.40	Contact, SV3
V82	0.747	16.505	0.912	0.24	0.25	Contact
V83	0.622	17.625	0.948	0.28	0.25	Contact
V85	0.283	17.636	1.239	0.36	0.41	Contact
V86	0.325	17.949	1.090	0.48	0.50	Contact
V87	0.369	17.140	1.117	0.24	0.26	Contact
V88	0.452	17.698	1.122	0.44	0.46	Contact
V89	0.456	18.486	0.836	0.34	0.34	Contact
V90	0.726	18.523	0.973	0.30	0.34	Contact
V91	0.457	19.518	1.103	0.70	0.70	Contact
V92	0.577	18.581	0.945	0.34	0.39	Contact
V100	1.66	16.966	0.846	1.05	1.15	Detached
V101	3.50	18.319	1.204	1.75	1.80	Detached
V103	0.673	18.411	0.931	0.23	0.25	Contact
V104	0.735	19.407	1.243	1.05	1.15	Contact

Table 11. Mean Properties of Suspected Variables

ID	Period	$\langle V \rangle$	$(B-V)_{\text{mag}}$	A_V	A_B	$\Delta\alpha$	$\Delta\delta$
SV10	0.376	17.666	1.028	0.10	0.11	-29.4	169.8
SV11	0.474	17.707	1.051	0.14	0.15	388.5	206.0
SV12	0.860	17.572	0.862	0.10	0.12	-11.1	-72.8
SV13	1.11	16.548	1.483	0.17	0.17	136.9	323.5
SV14	0.55	17.348	0.891	0.30	0.46	-28.7	-21.3
SV15	0.61	16.808	0.892	0.40	0.40	-26.4	-0.9

Table 12. Cluster properties

Cluster	Type	[Fe/H]	$\langle P_{ab} \rangle$	$\langle P_c \rangle$	N_c/N_{RR}
M3	Oo I	–1.6	0.56	0.32	0.16
M15	Oo II	–2.2	0.64	0.38	0.48
NGC 6441	?	–0.5	0.75	0.38	0.31

Table 13. RRc Parameters

ID	M/M_{\odot}	$\log(L/L_{\odot})$	T_{eff}	M_V
V70	0.53	1.68	7388	0.79
V71	0.36	1.64	7435	0.76
V72	0.48	1.65	7431	0.82
V73	0.49	1.66	7388	0.77
V74	0.43	1.63	7458	0.82
V77	0.36	1.64	7351	0.78
V78	0.41	1.65	7374	0.76
Mean	0.47 ± 0.05	1.65 ± 0.02	7408 ± 35	0.79 ± 0.03

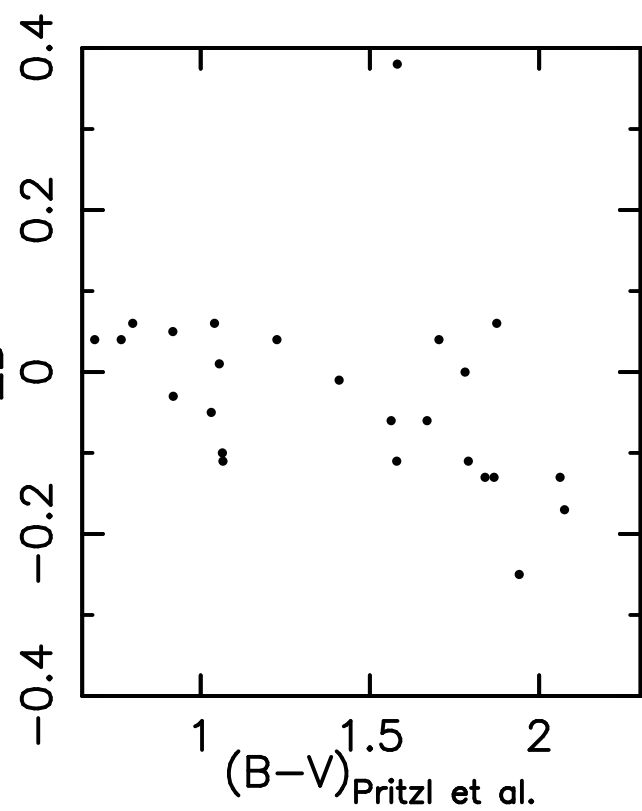
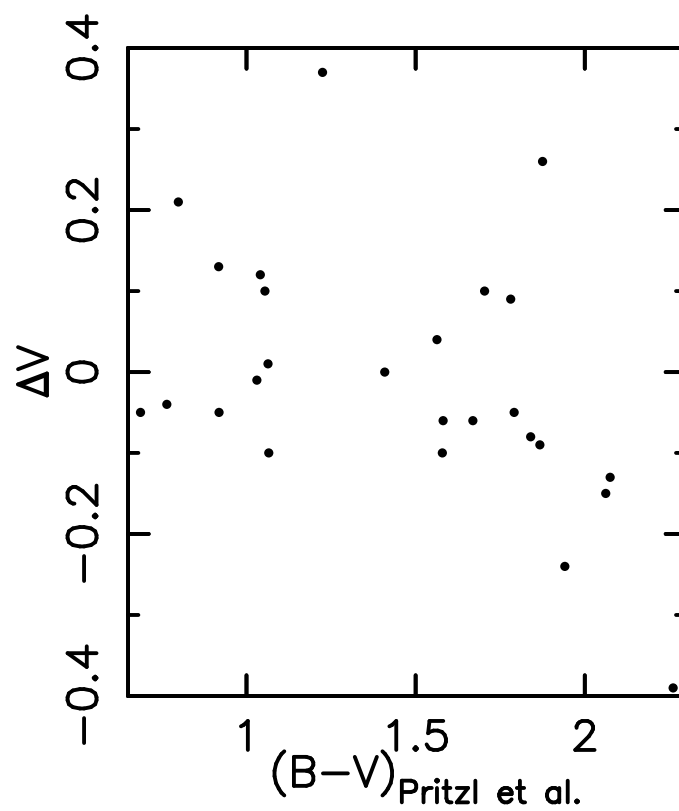
Note. — The mean was calculated excluding V71 and V77.

Table 14. RRab Parameters

ID	M/M_{\odot}	$\log(L/L_{\odot})$	$\log T_{\text{eff}}$	M_V	[Fe/H]
V37	0.54	1.63	3.83	0.74	-0.95
V38	0.55	1.69	3.81	0.66	-1.14
V40	0.54	1.66	3.82	0.71	-1.01
V43	0.55	1.69	3.81	0.65	-1.16
V51	0.53	1.65	3.82	0.67	-0.84
V55	0.53	1.65	3.82	0.68	-0.80
V57	0.55	1.66	3.82	0.69	-1.04
V59	0.53	1.65	3.82	0.69	-0.89
V61	0.55	1.66	3.81	0.65	-1.08
Mean	0.54	1.66	3.82	0.68	-0.99

Table 15. M15 Compatibility Condition

ID	D_m	Light Curve Source
02	3.580	Silbermann & Smith (1995)
09	4.795	Silbermann & Smith (1995)
08	4.423	Bingham et al. (1984)
12	5.500	Bingham et al. (1984)
25	5.628	Bingham et al. (1984)



This figure "Pritzl.fig02.gif" is available in "gif" format from:

<http://arxiv.org/ps/astro-ph/0107341v1>

This figure "Pritzl.fig03a.gif" is available in "gif" format from:

<http://arxiv.org/ps/astro-ph/0107341v1>

This figure "Pritzl.fig03b.gif" is available in "gif" format from:

<http://arxiv.org/ps/astro-ph/0107341v1>

This figure "Pritzl.fig03c.gif" is available in "gif" format from:

<http://arxiv.org/ps/astro-ph/0107341v1>

This figure "Pritzl.fig03d.gif" is available in "gif" format from:

<http://arxiv.org/ps/astro-ph/0107341v1>

This figure "Pritzl.fig03e.gif" is available in "gif" format from:

<http://arxiv.org/ps/astro-ph/0107341v1>

This figure "Pritzl.fig03f.gif" is available in "gif" format from:

<http://arxiv.org/ps/astro-ph/0107341v1>

This figure "Pritzl.fig03g.gif" is available in "gif" format from:

<http://arxiv.org/ps/astro-ph/0107341v1>

This figure "Pritzl.fig03h.gif" is available in "gif" format from:

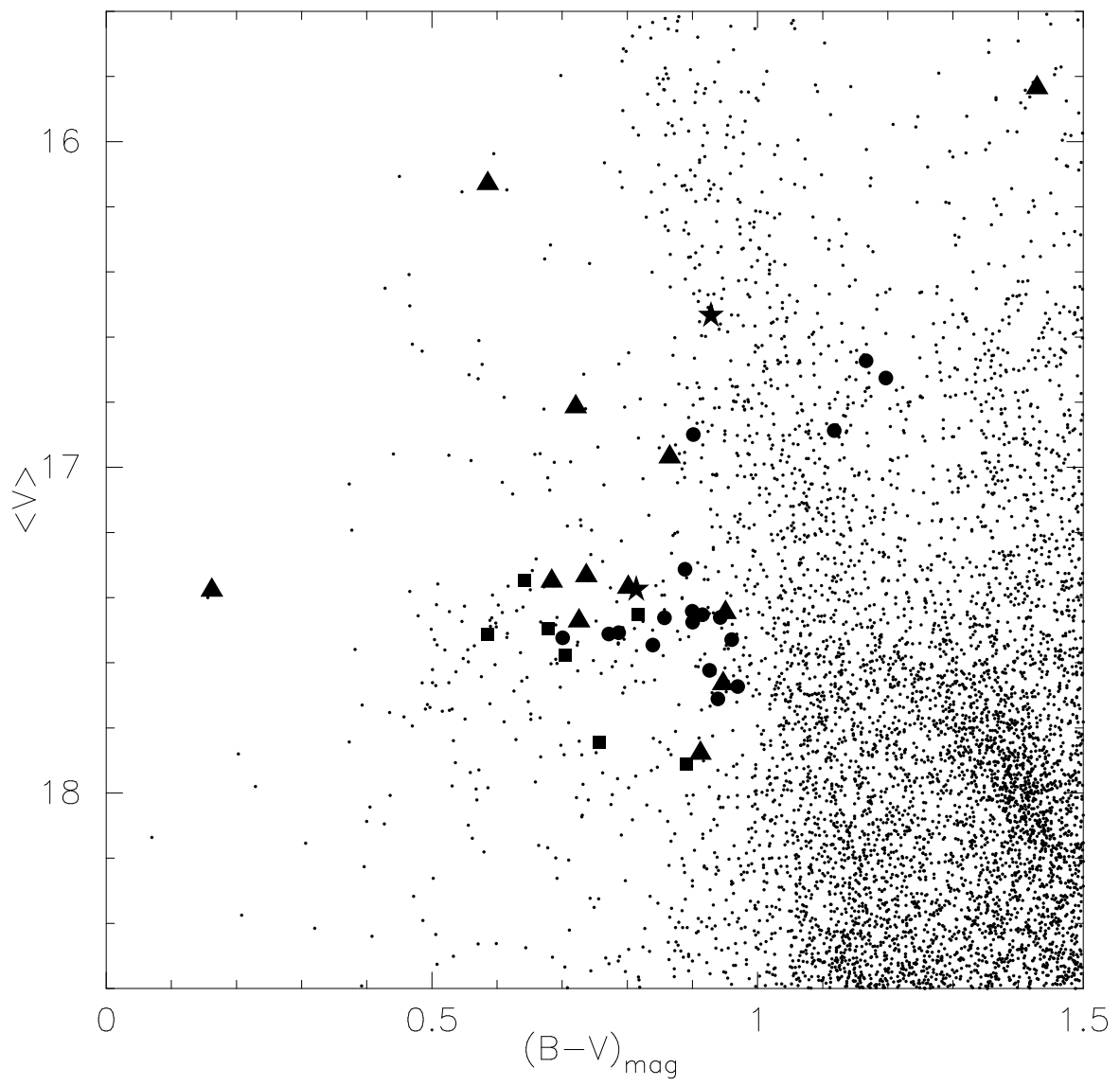
<http://arxiv.org/ps/astro-ph/0107341v1>

This figure "Pritzl.fig03i.gif" is available in "gif" format from:

<http://arxiv.org/ps/astro-ph/0107341v1>

This figure "Pritzl.fig03j.gif" is available in "gif" format from:

<http://arxiv.org/ps/astro-ph/0107341v1>



This figure "Pritzl.fig05a.gif" is available in "gif" format from:

<http://arxiv.org/ps/astro-ph/0107341v1>

This figure "Pritzl.fig05b.gif" is available in "gif" format from:

<http://arxiv.org/ps/astro-ph/0107341v1>

This figure "Pritzl.fig05c.gif" is available in "gif" format from:

<http://arxiv.org/ps/astro-ph/0107341v1>

This figure "Pritzl.fig05d.gif" is available in "gif" format from:

<http://arxiv.org/ps/astro-ph/0107341v1>

This figure "Pritzl.fig05e.gif" is available in "gif" format from:

<http://arxiv.org/ps/astro-ph/0107341v1>

This figure "Pritzl.fig05f.gif" is available in "gif" format from:

<http://arxiv.org/ps/astro-ph/0107341v1>

